Validation of Thiosemicarbazone Compounds as P-Glycoprotein Inhibitors in Human Primary Brain-Blood Barrier and Glioblastoma Stem Cells

Validation of thiosemicarbazone compounds as P-glycoprotein inhibitors in human primary brain-blood barrier and glioblastoma stem cells

Journal:	*Molecular Pharmaceutics*
Manuscript ID	mp-2019-00018a.R2
Manuscript Type:	Article
Date Submitted by the Author:	n/a
Complete List of Authors:	Salaroglio, Iris; Universita degli Studi di Torino, Dipartimento di Oncologia Abate, Carmen; Universita degli Studi di Bari Aldo Moro, Farmacia-Scienze del Farmaco Rolando, Barbara; Università degli Studi di Torino, Dipartimento di Scienza e Tecnologia del Farmaco Battaglia, Luigi; Università degli Studi di Torino Gazzano, Elena; Universita degli Studi di Torino, Dipartimento di Oncologia Colombino, Elena; Università di Torino, Dipartimento di Scienze Veterinarie Costamagna, Costanzo; Universita degli Studi di Torino, Dipartimento di Oncologia Annovazzi, Laura; Centro Ricerche, Fondazione Policlinico di Monza Mellai, Marta; Università del Piemonte Orientale, Dipartimento di Scienze della Salute Berardi, Francesco; Università degli Studi di Bari Aldo Moro , Dipartimento di Farmacia-Scienze del Farmaco Capucchio, Maria Teresa; Università di Torino, Dipartimento di Scienze Veterinarie Schiffer, Davide; Università degli Studi di Torino, Dipartimento di Neuroscienze Riganti, Chiara; Universita degli Studi di Torino, Dipartimento di Onoclogia

Validation of thiosemicarbazone compounds as P-glycoprotein inhibitors in human primary brain-blood barrier and glioblastoma stem cells

Iris Chiara Salaroglio[1], Carmen Abate[2], Barbara Rolando[3], Luigi Battaglia[3], Elena Gazzano[1], Elena Colombino[4], Costanzo Costamagna[1], Laura Annovazzi[5], Marta Mellai[6], Francesco Berardi[2], Maria Teresa Capucchio[4], Davide Schiffer[7], Chiara Riganti[1,*]

[1] Dipartimento di Oncologia, Università di Torino, via Santena 5/bis, 10126, Torino Italy

[2] Dipartimento di Farmacia-Scienze del Farmaco, Università di Bari "Aldo Moro", Via Orabona 4, 70125, Bari, Italy

[3]Dipartimento di Scienza e Tecnologia del Farmaco, via Pietro Giuria 9, 10125, Torino, Italy

[4] Dipartimento di Scienze Veterinarie, Università di Torino, Largo Braccini 2, 10095, Grugliasco, Italy

[5] Centro Ricerche, Fondazione Policlinico di Monza, via Pietro Micca 29, 13100, Vercelli, Italy

[6] Dipartimento di Scienze della Salute, Università del Piemonte Orientale, corso Mazzini 18, 28100, Novara, Italy

[7] Dipartimento di Neuroscienze, Università di Torino, via Cherasco 15, 10126, Torino

*** Corresponding author:** Dr. Chiara Riganti, Dipartimento di Oncologia, Università di Torino, via Santena 5/bis, 10126, Torino Italy; phone: +390116705857; fax: 390116705845; email: chiara.riganti@unito.it

Table of contents

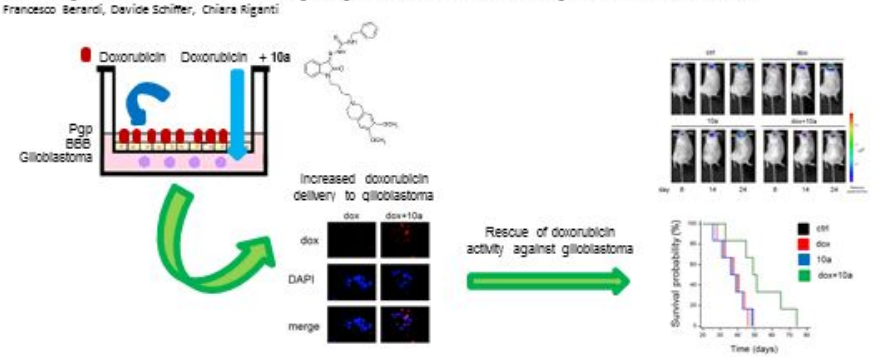

Abstract

P-glycoprotein (Pgp) is highly expressed on blood-brain barrier (BBB) cells and glioblastoma (GB) cells, in particular on cancer stem cells (SC). Pgp recognizes a broad spectrum of substrates, limiting the therapeutic efficacy of several chemotherapeutic drugs in eradicating GB SC. Finding effective and safe inhibitors of Pgp that improve drug delivery across BBB and target GB SC is open to investigations.

We previously identified a series of thiosemicarbazone compounds that inhibit Pgp with an EC_{50} in the nanomolar range and herein we investigate the efficacy of three of them in bypassing the Pgp-mediated drug efflux in primary human BBB and GB cells.

At 10 nM concentration the compounds were not cytotoxic for brain microvascular endothelial hCMEC/D3 cell line, but they markedly enhanced the permeability of the Pgp-substrate doxorubicin through BBB. Thiosemicarbazone derivatives increased doxorubicin uptake in GB, with greater effects in the Pgp-rich SC clones than in the differentiated clones derived from the same tumor. All the compounds increased intratumor doxorubicin accumulation and consequent toxicity in GB growing under competent BBB, producing a significant killing of GB SC. The compounds crossed the BBB monolayer. The most stable derivative, compound **10a**, had a half-life in serum of 4.2 h. The co-administration of doxorubicin plus compound **10a** significantly reduced the growth of orthotopic GB-SC xenografts, without eliciting toxic side-effects.

Our work suggests that the thiosemicarbazone compounds are able to transform doxorubicin, a prototype of BBB-impermeable drug, into a BBB-permeable drug. Bypassing the Pgp-mediated drug efflux in both BBB and GB SC, thiosemicarbazones might increase the success of chemotherapy in targeting GB SC, which represent the most aggressive and difficult components to be eradicated.

Keywords: glioblastoma multiforme; cancer stem cell; blood-brain barrier; P-glycoprotein; thiosemicarbazones

Abbreviations: GB, glioblastoma multiforme; CNS, central nervous system; BBB, blood-brain barrier; SC, stem cell; ABC, ATP binding cassette; Pgp/ABCB1, P-glycoprotein; MRP1/ABCC1, multidrug-resistance related protein 1; BCRP/ABCG2, breast cancer resistance protein; BAT, brain-adjacent to tumor; TEER; transendothelial electrochemical resistance; FITC, fluorescein isothiocyanate; AC, adherent cells; NS, neurospheres; LDH, lactate dehydrogenase; DAPI; 4′,6-diamidino-2-phenylindole dihydrochloride; DAB, 3,3′-diaminobenzidine tetrahydrochloride.

Introduction

The pharmacological treatment of glioblastoma multiforme (GB), the most common brain tumor in the adult population, is hampered by the muticlonality of the tumor, the constitutive resistance to a broad spectrum of chemotherapeutic drugs, the surrounding blood-brain barrier (BBB). [1,2]

The cancer stem cell (SC) component within GB mediates tumor chemoresistance, for the high activity of DNA-repairing systems, the constitutive activation of pro-survival and anti-apoptotic pathways, the presence of hypoxic and growth factors-rich niches.[3,4] Moreover GB SC are rich of drug efflux transporters belonging to the ATP binding cassette (ABC) family, such as P-glycoprotein (Pgp/ABCB1), multidrug-resistance related protein 1 (MRP1/ABCC1), breast cancer resistance protein (BCRP/ABCG2) that efflux different chemotherapeutic agents (e.g. doxorubicin, etoposide, carmustine, vincristine and temozolomide). [4,5,6]

BBB, that surrounds brain parnechyma, is a second obstacle for chemotherapy success in GB: indeed, in BBB there are no fenestrations and pinocytic vesicles, and high levels of tight junctions, adherent junctions and ABC transporters. [8,9] The BBB is disrupted within the bulk of GB, but it is preserved in the so-called "brain-adjacent to tumor" (BAT) area. Here, sporadic clusters of GB cells can be responsible for local relapse or spreading in other central nervous system (CNS) areas if not eliminated by chemotherapy.[8] Pgp is present on the luminal side of BBB and induces the brain-to-blood efflux of chemotherapeutic drugs (doxorubicin, taxanes, Vinca alkaloids, teniposide/etoposide, topotecan, methotrexate) and targeted-therapies (imatinib, dasatinib, lapatinib, gefitinib, sorafenib, erlotinib).[9]

Pgp in both BBB and GB constitutes a "double barrier" that dramatically reduces the success of chemotherapy against this tumor. Strategies aimed to inhibit Pgp increasing drug delivery across BBB [10-15] and within GB [16-18] are under intensive investigation. To date, however, there are no satisfactory tools that bypass the Pgp-drug efflux mediated in both BBB and GB cells, in particular in SC component.

Recently, we synthesized a series of thiosemicarbazone derivatives as inducers of collateral sensitivity, i.e. compounds with a higher cytotoxicity against Pgp-overexpressing tumors than against Pgp-negative ones.[19] In the compounds' design, a multitarget strategy was adopted: a metal chelator portion was connected to a moiety targeting both sigma-2 receptor and Pgp [20], in order to couple the antiproliferative activity due to the activation of sigma-2 receptor to the iron chelation and Pgp modulation.[21,22] Within this library, three compounds - namely compound **8a**, **10a** and **17a** - emerged for their inhibitory activity of Pgp at nanomolar concentration, in line with the most potent Pgp blockers such as PSC833 or Tariquidar. On the other hand, the compounds were not cytotoxic in this concentration range in the investigated cell lines (breast MCF7 and lung A549 cancer cells), having an IC_{50} on cell viability in the micromolar range.[20] Owing to these two features, these three thiosemicarbazones may hold promises as potentially effective and safe Pgp inhibitors.

In the present work we validated these compounds as potential Pgp inhibitors at both BBB and GB level. We investigated their ability to transform doxorubicin, a prototypical Pgp substrate that is not delivered across BBB [13,23] and does not kill GB SC [17], into a drug with good intratumor delivery and efficacy against primary GB SC growing under BBB.

Experimental Section

Chemicals. Sterile materials for cell cultures was from Falcon (Becton Dickinson, Franklin Lakes, NJ). Reagents for electrophoresis and materials for immunoblotting were from Bio-Rad Laboratories (Hercules, CA). Protein amounts were measured by the BCA kit from Sigma Chemicals Co. (St. Louis, MO). If not specified differently, the reagents were from Sigma Chemicals Co.

Synthesis and characterization of compounds. Compounds **8a** ((*Z*)-2-(1-(4-(6,7-Dimethoxy-3,4-dihydroisoquinolin-2(1*H*)-yl)butyl)-2-oxoindolin-3-ylidene)-*N*-*i*-propylhydrazinecarbothioamide hydrochloride), **10a** ((*Z*)-2-(1-(4-(6,7-Dimethoxy-3,4-dihydroisoquinolin-2(1*H*)-yl)butyl)-2-oxoindolin-3-ylidene)-*N*-benzylhydrazinecarbothioamide hydrochloride) and **17a** ((*Z*)-2-(1-(4-(6,7-

Dimethoxy-3,4-dihydroisoquinolin-2(1*H*)-yl)butyl)-2-oxoindolin-3-ylidene)-*N*-(naphthalen-1-yl)-hydrazinecarbothioamide hydrochloride) were synthesized as reported.[20] The chemical structure is shown in **Figure 1**. Calcein-acetoxy methylester (AM) assay and ATP assays were used to mesure Pgp activity. [20,24]

Figure 1

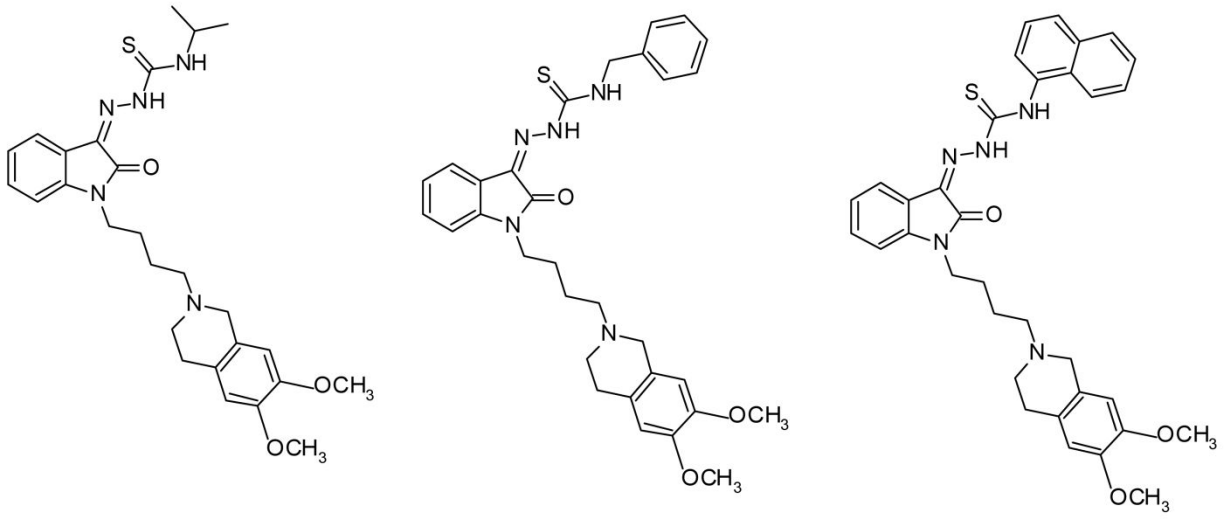

8a **10a** **17a**

Cells. hCMEC/D3 cells, a human brain microvascular endothelial stabilized cell line (provided by Prof. Pierre-Olivier Couraud, Institut Cochin, Centre National de la Recherche Scientifique UMR 8104, INSERM U567, Paris, France), were cultured in Transwell devices (0.4 μm diameter pores-size, Corning Life Sciences, Chorges, France) for 7 days until the confluence. [23] The transendothelial electrochemical resistance (TEER), considered a parameter of BBB integrity (measured with a Voltohmetro Millicell-ERS (Millipore, Billerica, MA), and the permeability coefficients of dextran-fluorescein isothiocyanate (FITC), [^{14}C]-sucrose, and [^{14}C]-inulin, considered parameters of paracellular transport, [13] were measured before each experiments, giving the following results: TEER value: 28-38 Ω cm^2; dextran-FITC permeability coefficient: 0.019 ± 0.004 × 10^{-3} cm min^{-1}; [^{14}C]-sucrose permeability coefficient: 1.28 ± 0.19 × 10^{-3} cm min^{-1}; [^{14}C]-inulin permeability coefficient: 0.45 ± 0.07 × 10^{-3} cm min^{-1}. These data are indicative of a competent hCMEC/D3 monolayer, in lines with previous finidngs. [23]

Primary human GB cells (01010627, CV17) of patients were collected during surgical procedures at the Neurosurgical Unit, Universities of Torino, Italy, and from DIBIT San Raffaele, Milan, Italy (Dr. Rossella Galli). GB histological diagnosis was performed following WHO guidelines. Cells were cultured as adherent cells (AC) or neurospheres (NS), considered a reliable in vitro model of GB SC component, [25] with minor changes.[17] Morphological analysis, evaluation of differentiation and stemness markers, functional stemness assays (*in vitro* clonogenicity and self-renewal, *in vivo* tumorigenicity) are reported in [17,26] and in **Supplementary Table 1**.

In co-culture systems, hCMEC/D3 cells were seeded in the Transwell insert; after 4 days, 500,000 GB cells were added in the lower chamber. Coc-ultures were maintained for 3 days further, then the medium of upper and lower chamber was canged, and cells were subjected to the assays indicated below.

Cytotoxicity. The release of lactate dehydrogenase (LDH) in culture medium, a parameter of cells damage and necrosis [27], was measured spectrophotometrically. [17] Intracellular and extracellular LDH activity were expressed as μmol NADH oxidized/min/dish; extracellular LDH activity was calculated as percentage of (intracellular + extracellular) LDH activity in the dish. In co-culture systems, 5 μM doxorubicin was added to the Transwell inserts. After 24 h, medium and GB cells from the lower chamber were collected, and checked for the activity of LDH. Cell viability was evaluated by the ATPlite Luminescence Assay System (PerkinElmer, Waltham, MA), as per manufacturer's instructions. The relative luminescence units (RLUs) of untreated cells were considered corresponding to 100% viability; the results were expressed as a percentage of viable cells versus untreated cells.

Doxorubicin uptake. The uptake of doxorubicin in hCMEC/D3 and GB cells [26] and the intratumor delivery of doxorubicin in co-culture systems [12] were measured fluorimetrically. Accumulation of doxorubicin within GB cells growing under BBB were also analyzed by fluorescence microscopy [26], in cells fixed with 4% w/v paraformaldehyde and labelled with 4′,6-diamidino-2-phenylindole

dihydrochloride (DAPI) to counterstain the nuclei, using a Leica DC100 fluorescence microscope (Leica Microsystems GmbH, Wetzlar, Germany). For each experimental point, a minimum of 5 microscopic fields were examined.

Rhodamine 123 uptake. The intracellular retention of rhodamine 123 in hCMEC/D3 cells, an additional parameter of Pgp activity, was measured as fluorimetrically [13] and expressed as nmol/mg cell proteins.

Thiosemicarbazone derivatives quantification. To measure the cellular uptake of thiosemicarbazone derivatives, confluent hCMEC/D3 cells grown 7 days in Transwell devices, were incubated 3 h with 10 nM of compounds **8a**, **10a** and **17a**. Cells were washed twice with PBS, detached, sonicated and re-suspended in 0.7 ml PBS. 0.2 ml were used to assess the protein content, 0.5 ml were used to measure the concentration of thiosemicarbazones. To measure the concentration of **10a** in serum, 0.5 ml peripheral blood was collected after animals euthanasia, incubated 30 minute at room temperature and centrifuged at 1,500 g for 10 minutes at 4°C. Samples were added to 0.5 ml of 0.1% v/v HCOOH, dissolved in acetonitrile to deproteinize the serum, vortexed, sonicated for 3 min and centrifuged at 2,500 x g for 5 min. The supernatant, filtered through 0.45 µm PTFE-filters, was analyzed by RP-HPLC, using a HP 1100 chromatograph system (Agilent Technologies, Palo Alto, CA), equipped with a quaternary pump (model G1311A), a membrane degasser (G1379A), a diode-array detector (model G1315B) and a Nucleosil Nautilus analytical column (4.6 × 250 mm, 5 µm; Macherey-Nagel, Düren, Germany). The mobile phase consisting of acetonitrile 0.1% HCOOH v/v (solvent A) and water 0.1% HCOOH v/v (solvent B) at a flow rate of 1.0 ml/min with gradient conditions: 45% A until 4 min, from 45 to 60% A between 4 and 8 min, 60% A between 8 and 12 min, and from 60 to 45% A between 12 and 15 min. The column effluent was monitored at 365 nm, with a 800 nm reference wavelength. Data were analysed using a HP ChemStation system (Agilent Technologies), after performing a calibration curve in 5 nM-50 µM concentration range (r^2=0.996). Results were expressed as nanmol/mg cell proteins or nanomol/ml serum.

Permeability assays. The permeability of doxorubicin (parameter of Pgp and MRP1 activity [23]), mitoxantrone (parameter of BCRP activity [23]), dextran-FITC (parameter of tight junction integrity [28]), was measured as detailed previously.[13] The permeability coefficients were calculated as reported.[29] To measure the permeability of thiosemicarbazone compounds, each compound was incubated at the final concentration of 10 nM in insert of a Transwell device. After 3 h, the amount of compounds in the medium of the lower chamber was determined by RP-HPLC, as reported above. The results were expressed as percentage of concentration of each compound in the lower chamber/concentration of each compound in the insert at t_0 and as permeability coefficient. [29]

Immunoblotting. Twenty μg protein extracted with ice-cold lysis buffer (50 mM, Tris, 10 mM EDTA, 1% v/v Triton-X100), containing the protease inhibitor cocktail set III (Calbiochem, San Diego, CA), 2 mM phenylmethylsulfonyl fluoride and 1 mM Na_3VO_4, were resolved by SDS-PAGE and immunoblotted for Pgp (C219; Calbiochem), MRP1 (MRPm5; Abcam, UK), BCRP (M-70; Santa Cruz Biotechnology Inc., Santa Cruz, CA), claudin 3 (PA5-16867; ThermoFisher Scientific, Waltham, MA), claudin 5 (4C3C2; ThermoFisher Scientific), occludin (6HCLC; ThermoFisher Scientific), zonula occludens-1 ZO1 (40-2200; ThermoFisher Scientific), β-tubulin (D-10; Santa Cruz Biotechnology Inc.), followed by a peroxidase-conjugated secondary antibody (Bio-Rad Laboratories). After washing with Tris-buffered saline-Tween 0.1% v/v solution, the proteins were detected by enhanced chemiluminescence (Bio-Rad Laboratories).

Serum stability. 50 μM of compounds, dissolved in DMSO, were added to human serum (sterile-filtered from human male AB plasma, Sigma) at 37 °C, shaken for 24 h and at fixed time points within 24 h, 200 μl of the samples were analyzed by RP-HPLC, as detailed above. The half-life ($t_{1/2}$) of the compounds was determined by fitting the data with one phase exponential decay equation using Prism software v5 (Graph Pad, San Diego, CA).

In vivo tumor growth and histopathological analysis. 1×10^6 NS cells, re-suspended in 150 μl sterile physiological solution, stably transfected with the pGL4.51[luc2/CMV/Neo] vector (Promega

Corporation), were stereotactically injected into the right caudatus nucleus into 6-8 week old female BALB/c *nu*/*nu* mice (weight: 20.3 g ± 2.4), anesthetized with sodium phenobarbital (60 mg/kg) intraperitoneally (i.p.) Tumor growth was monitored by *in vivo* bioluminescence (Xenogen IVIS Spectrum, PerkinElmer, Waltham, MA) 6, 14 and 24 days post-implantation. At day 7, animals were randomized (6 animals/group) and treated once/week for 3 weeks as reported: 1) control group, treated with 200 µl saline solution intravenously (i.v.); 2) doxorubicin group, treated with 5 mg/kg doxorubicin (dissolved in 100 µl aqueous solution) i.v.; 3) **10a** group, treated with 10 nM compound **10a** (dissolved on 100 µl aqueous solution with 1% DMSO) i.v.; 4) doxorubicin+ compound **10a** group, treated with 5 mg/kg doxorubicin + 10 nM compound **10a** i.v. Animals were euthanized at day 25 or if they showed signs of significantly compromised neurological function or loss of body weight >20%. Hemocromocytometric analyses, performed on 500 µl of blood collected after euthanasia, were assessed with a UniCel DxH 800 Coulter Cellular Analysis System (Beckman Coulter, Miami, FL), with commercial kits from Beckman Coulter Inc.

In a second cohort of mice, animals with orthotopic tumors were monitored until their spontaneous exitus or the onset of a situation determining euthanasia. Overall survival was the interval between tumor implant and exitus/euthanasia.

In a third experimental set, animals without tumors were treated as reported above and sacrificed after 24 h and 7 days. The concentration of **10a** in the serum was measured by RP-HPLC. Brain were collected and used for doxorubicin quantification or histopathological analysis. Doxorubicin was evaluated in OCT-embedded 10 µm sections by fluorescence microscopy, as detailed above. For histopathological analyses, paraffin-embedded 5 µm slide sections of cerebral and cerebellar cortex were stained with hematoxylin and eosin or immuno-stained with an anti-cleaved caspase-3 antibody (ab49822, Abcam), followed by the Vectastain ABC-AP Kit Universal (Vector Laboratoires, Burlingame, CA). After heating sections at 98 °C for 25 min in citrate buffer for antigen retrieval, 3% v/v H_2O_2 was added for 5 min to quench endogenous peroxidase activity. Primary antibody was added fir 2 h in a humidified chamber at 4 °C with the primary antibody, biotinylated link antibody

and peroxidase-labeled streptavidin were added for 10 min followed by 3,3′-diaminobenzidine tetrahydrochloride (DAB). Nuclei were counterstained with hematoxylin. For each sample, a minimum of 5 microscopic fields were examined.

Animal care and experimental procedures were approved by the Bio-Ethical Committee of the Italian Ministry of Health (#122/2015-PR).

Doxorubicin biodistribution. BALB/c *nu*/*nu* mice (6 animals/group) were treated with 200 µl saline solution i.v. ("ctrl" group), 5 mg/kg doxorubicin (dissolved in 100 µl aqueous solution) i.v., 5 mg/kg doxorubicin + 10 nM compound **10a** (dissolved on 100 µl aqueous solution with 1% DMSO) i.v. Animals were euthanized 0.5, 3, 6 and 24 h after treatments. Blood, brain, liver, spleen, heart, kidneys and lungs were collected. Tissues were fixed in 0.4% v/v paraformaldehyde for 18 h, washed with PBS, minced into 1 mm^3-pieces, rinsed with 1 ml ethanol/HCl 0.3 N, homogenized for 30 s at 15 Hz, using a TissueLyser II device (Qiagen, Hilden, Germany). An aliquot of samples was used for protein measurement; the remaining part was used for the fluorimetric doxorubicin measurement. Plasma, obtained by centrifuging blood at 1,500 g for 15 min at 4°C, was used both for protein determination and doxorubicin quantification, after diluting sample 1:1 in ethanol/HCl 0.3 N. The fluorescence of blood and organs in animals treated with saline solution (i.e. the intrinsic auto-fluorescence), was subtracted from the fluorescence of the corresponding sample of treated mice. Results were expressed as nmol/mg protein.

Statistical analysis. All data in the text and figures are provided as means ± SD. The Statistical Package for Social Science (SPSS) software (IBM SPSS Statistics v.19) was used to perform one-way analysis of variance (ANOVA). Overall survival was calculated by the Kaplan-Meier method, the outcome of the each treated group was calculated with the log rank test, using MedCalc® software (v.17.4). $p < 0.05$ was considered significant.

Results

Thiosemicarbazones increases the permeability of Pgp substrates across BBB monolayer

We first evaluated the cytotoxicity of thiosemicarbazone inhibitors on intact BBB. All compounds displayed dose- and time-dependent cytotoxicity on hCMEC/D3 cells monolayer. At 10 and 100 nM - a concentration range compatible with their EC_{50} values on Pgp [20] - they did not induce a significant increase in the release of LDH from BBB cells after 3 and 6 h (**Figure 2A-C,** *left panels*), suggesting that they did not elicit a necrotic damage. A significant increase in LDH release was observed at 1 μM concentration, at each time points for compound **8a** and **10a**, and after 24 h for compound **17a**. Since in untreated hCMEC/D3 cells the release of LDH was not increased at the different time points evaluated, the increase observed in cells treated with thiosemicarbazone derivatives after 24 h was likely due to cytotoxicity exerted by the compounds. These data are in line with the cytotoxicity profile of thiosemicarbazones on cancer cell lines, where micromolar concentrations of compounds **8a**, **10a** and **17a** were cytotoxic.[20] In keeping with the release of LDH, the viability of hCMEC/D3 cells was reduced at each concentration after 24 h exposure. Only compound **10a** showed a decreased viability after 6 h of treatment (**Figure 2A-C,** *right panels*).

To avoid any bias due to the presence of a damaged BBB, all the following assays were performed using 3 h incubation and 10 nM concentration of each compound, i.e. adopting experimental conditions that did not induce necrotic damage nor reduce viability of BBB cells.

Figure 2

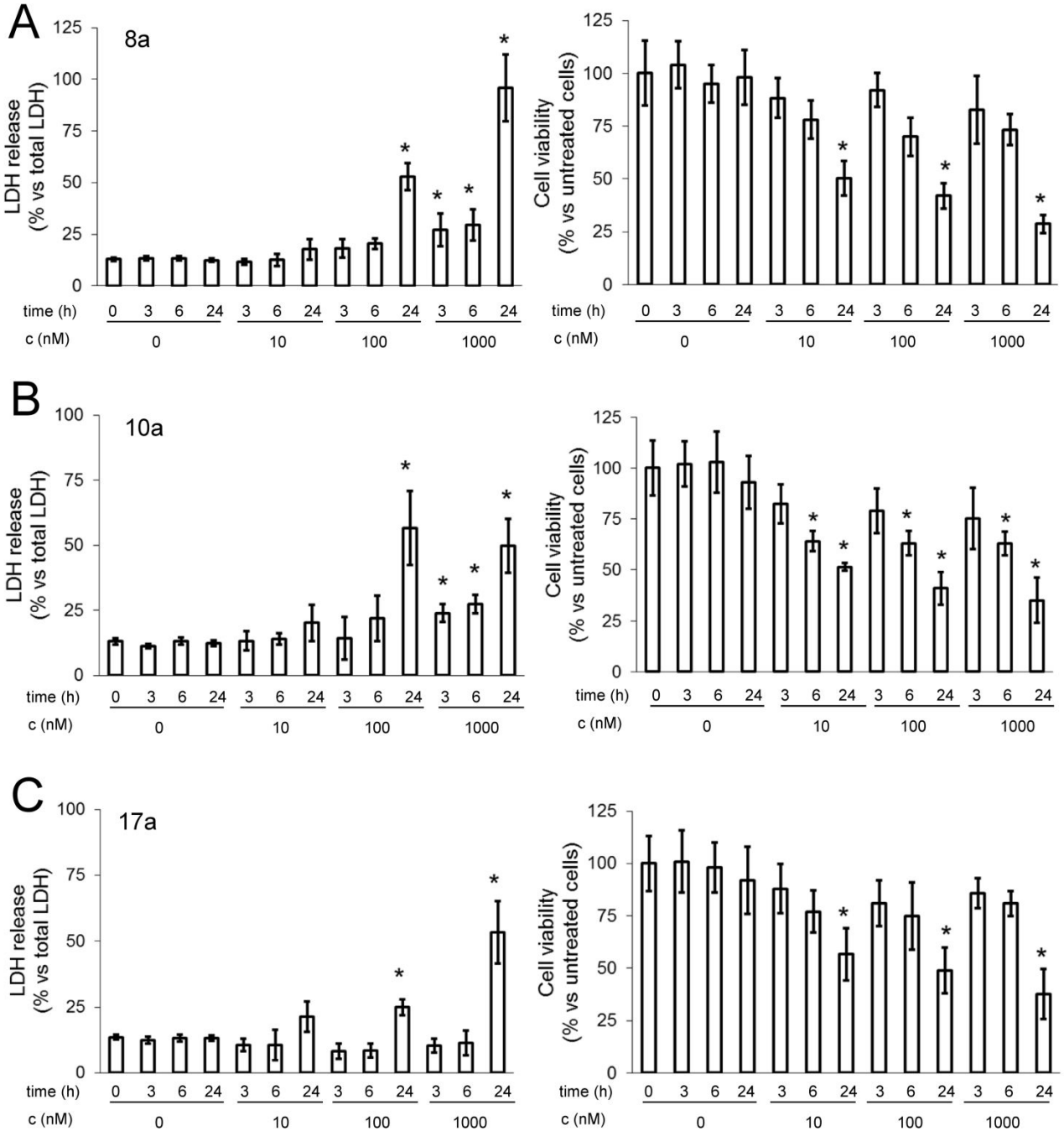

All the compounds significantly increased the uptake of doxorubicin (**Figure 3A**) and rhodamine 123 (**Figure 3B**) within hCMEC/D3 cells at 10 nM concentration, suggesting that at this concentration they effectively increased the retention of Pgp substrates within BBB cells. To measure if the uptake was followed by a trans-BBB permeability, we seeded hCMEC/D3 monolayers in the Transwell insert (upper chamber) and added **8a**, **10a** and **17a** compounds plus doxorubicin, mitoxantrone or

dextran-FITC, in contact with the BBB luminal side. After 3 h, we measured the amount of the above-indicated drugs in the medium of the lower chamber (**Figure 3C**). In line with the higher uptake, the doxorubicin's permeability across BBB monolayer was significantly increased (**Figure 3D**). Of note, the increase in doxorubicin permeability was comparable to the increase exerted by the Pgp inhibitor Elacridar, at a concentration (10 μM) able to fully inhibit Pgp activity. [30] The increased permeability was selective for Pgp substrates. Indeed, the compounds did not increase the permeability of the BCRP substrate mitoxantrone (**Figure 3E**). The permeability of dextran (**Figure 3F**), a compound that crosses BBB in case of loss of integrity, did not change and was in line with the value reported for a competent monolayer of hCMEC/D3 cells, [23] indicating that the tiosemicarbazone derivatives did not compromise BBB integrity of hCMEC/D3 monolayers. Also, the compounds did not modify TEER values (**Figure 3G**), suggesting that the activity of BCRP and the competence of tight junctions was not altered.

Figure 3

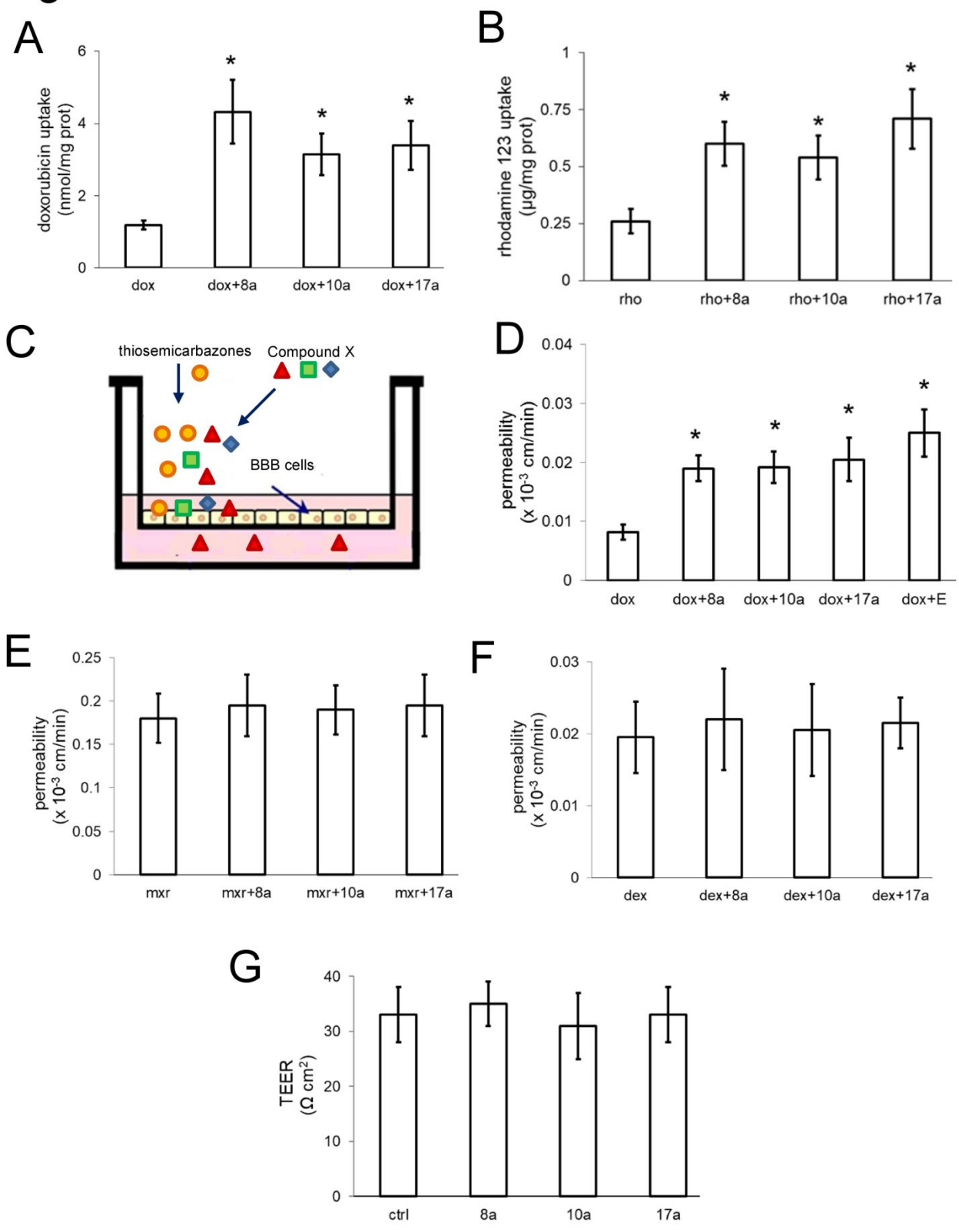

Moreover, in these experimental conditions the amount of Pgp, MRP1, BCRP, three ABC transporters involved in doxorubicin efflux [8], and tight junctions-related protein, was not modify by the

compounds (**Supplementary Figure 1**). Overall, these data suggested that peculiar effects of thiosmeicarbazone derivatives was a reduction in Pgp activity.

As shown in **Supplementary Figure 2A-B**, doxorubicin used alone did not elicit cell damage nor reduce cell viability, likely as a consequence of its fast efflux from BBB cells via Pgp. The anthracycline did not increase the toxicity of compounds **8a**, **10a** and **17a** (refer to Figure 2 as comparison), suggesting that the drug did not accumulate within BBB but was instead transported across the BBB in the presence of thiosemicarbazone derivatives.

Thiosemicarbazones increase doxorubicin intratumor delivery and efficacy against primary GB cells co-cultured with BBB cells

We next investigated if the increased delivery of doxorubicin across BBB monolayer produced an increased delivery of the drug within GB cells growing under BBB. To this aim, we used two primary GB stabilized cell lines, cultured as AC or NS populations. The former were relatively sensitive to doxorubicin *in vitro* [17] and had low or undetectable expression of Pgp, MRP1 and BCRP; the latter were doxorubicin-resistant [17] and had a basally high expression of these transporters (**Supplementary Figure 3**).

As expected, thiosemicarbazone derivatives did not increase the doxorubicin uptake in Pgp-poorly expressing GB AC cultured alone (i.e. in the absence of BBB), while they significantly increased doxorubicin retention in the Pgp-rich GB SC population (**Supplementary Figure 4A-B**).

We previously demonstrated that the presence of a competent BBB strongly reduces the intratumor delivery and efficacy of doxorubicin, because of the Pgp-mediated efflux of the drug by BBB cells.[13] To verify if the co-incubation with thiosemicarbazone derivatives improved doxorubicin delivery and cytotoxicity in GB cells growing under a competent BBB, we added doxorubicin and compounds **8a**, **10a** and **17a** – used a non-toxic concentration for BBB (Figure 2) –in the Transwell insert of the co-culture system, facing the Pgp expressed on the luminal side of BBB cells. In co-culture settings,

doxorubicin was poorly accumulated in GB cells growing in the lower chamber, i.e. under hCMEC/D3 monolayer (**Figure 4A-C**) and was not cytotoxic, as demonstrated by the lack of increase in the LDH release (**Figure 5A, C**) and by the lack of changes in cell viability (**Figure 5B, D**). In both primary GB samples, drug accumulation and toxicity was even lower in NS than in AC (**Figures 4-5**), as a consequence of the higher expression of Pgp in the former (**Supplementary Figure 3**). However, the thiosemicarbazone increased doxorubicin accumulation (**Figure 4A-C**) and release of extracellular LDH (**Figure 5A, C**), in AC and NS co-cultured under BBB. The small increase of LDH was paralleled by a reduction in cell viability (**Figure 5B, D**), suggesting that the damage produced by doxorubicin in GB cells was sufficient to induce cell death. Of note, the amount of intracellular doxorubicin, the release of LDH and the viability in NS-BBB co-cultures exposed to the compounds was the same as in AC-BBB co-cultures, suggesting that the thiosemicarbazone derivatives fully inhibited the Pgp present in NS.

Figure 4

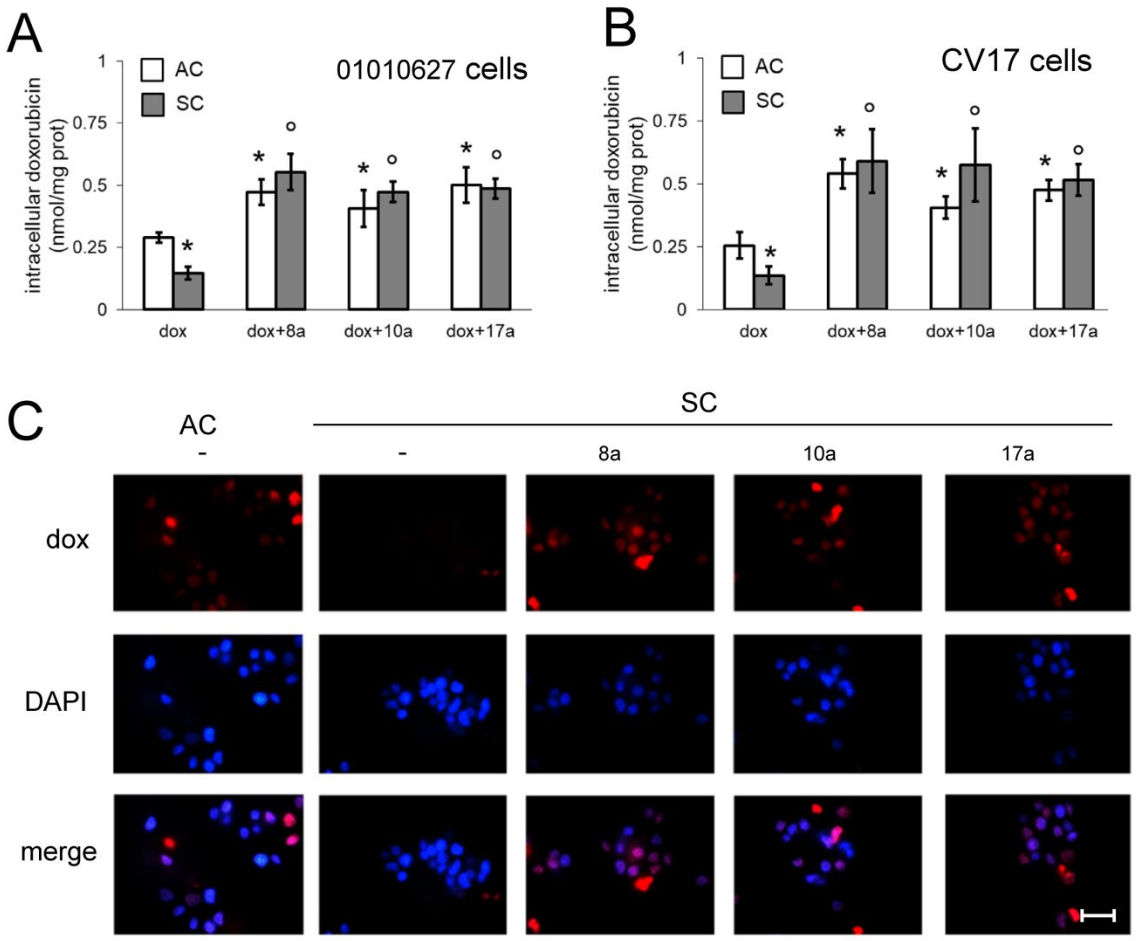
A
AC
SC
01010627 cells
intracellular doxorubicin (nmol/mg prot)
1
0.75
0.5
0.25
0
dox
dox+8a
dox+10a
dox+17a
B
AC
SC
CV17 cells
intracellular doxorubicin (nmol/mg prot)
dox
dox+8a
dox+10a
dox+17a
C
AC
SC
-
-
8a
10a
17a
dox
DAPI
merge

Figure 5

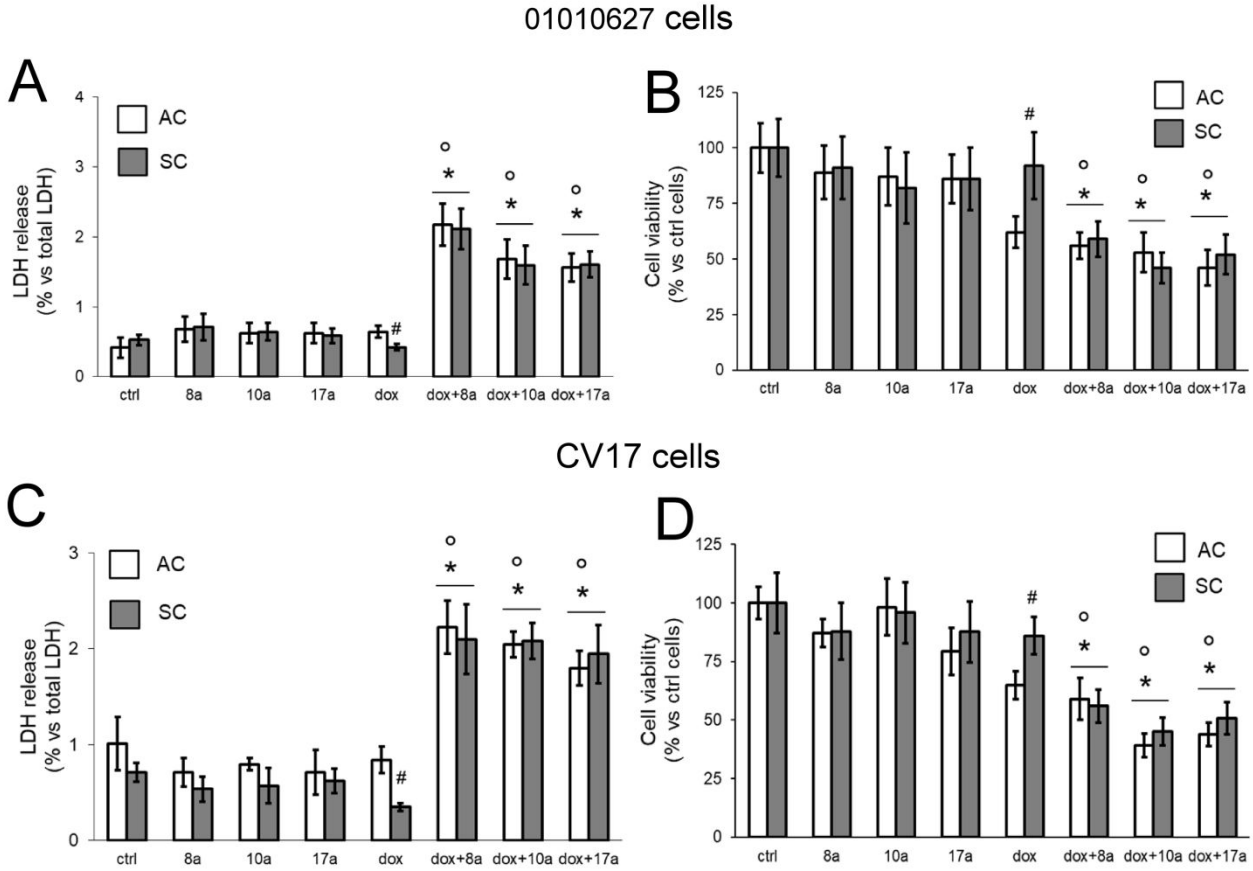

These experimental sets led to hypothesize that thiosemicarbazones may inhibit both the Pgp of the luminal side of BBB and the Pgp of GB SC, and that they likely cross BBB.

Thiosemicarbazones are BBB-permeant compounds

We thus measured the uptake and permeability of thiosemicarbazones across BBB monolayer: we incubated 10 nM of each compound in the insert of a Transwell device, facing the luminal side of BBB, rich of Pgp. After 3 h, compounds **8a**, **10a** and **17a** were detectable within BBB cells (**Figure 6A**) and in the lower chamber, with a percentage corresponding to 46.21 $\pm$ 8.05, 56.76 $\pm$ 2.23 and 41.72 $\pm$ 4.82, respectively, compared to the amount present at t0 in the upper chamber (**Figure 6B**). In Transwells without cells, the percentage of compounds recovered from the lower chamber medium was 88.08 $\pm$ 7.05 for **8a**, 86.85 $\pm$ 6.25 for **10a** and 91.08 $\pm$ 4.73 for **17a.** The high permeability

coefficient of the compounds (**Figure 6C**) indicated that they have a good delivery across hCMEC/D3 monolayer.

Figure 6

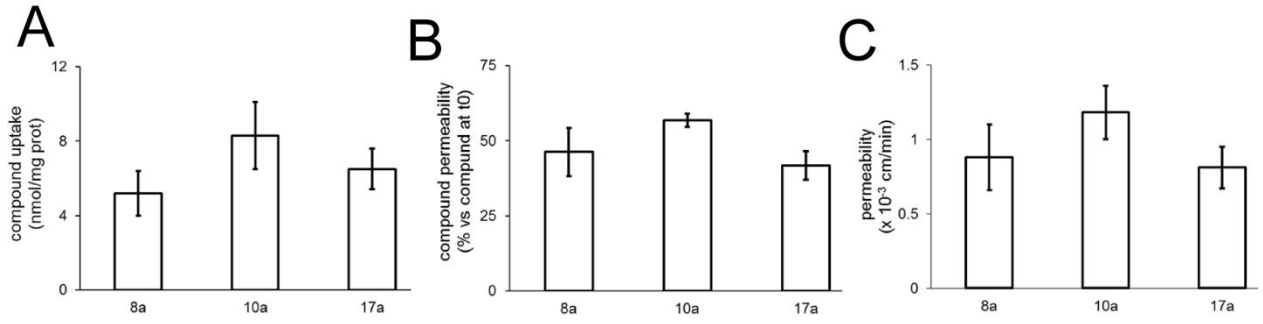

Thiosemicarbazones rescue the efficacy of doxorubicin against orthotopic patient-derived xenograft tumors

The half-life of the compounds in human serum was of 4.8 h for compound **8a**, 4.2 h for compound **10a** and 1.5 h for compound **17a** (**Figure 7A**). We thus focused on compound **10a**, that had highest permeability across the BBB (**Figure 6B-C**) and good serum stability (**Figure 7A**), and was effective in rescuing doxorubicin cytotoxicity in vitro.

Orthotopic implanted tumors derived by GB SC of 01010627 were completely refractory to doxorubicin: indeed the drug did not reduced tumor growth (**Figure 7B-C**), nor improved animal survival (**Figure 7D**). Animals treated with compound **10a** alone did not differ from the untreated animals. By contrast, the co-administration of doxorubicin and compound **10a** reduced tumor growth (**Figure 7B-C**) and improved the animal survival (**Figure 7D**). The median survival of each groups was: 38.5 days (ctrl group), 39.5 days (doxorubicin group), 37.5 days (**10a** group), 50 days (doxorubicin + **10a** group).

Figure 7

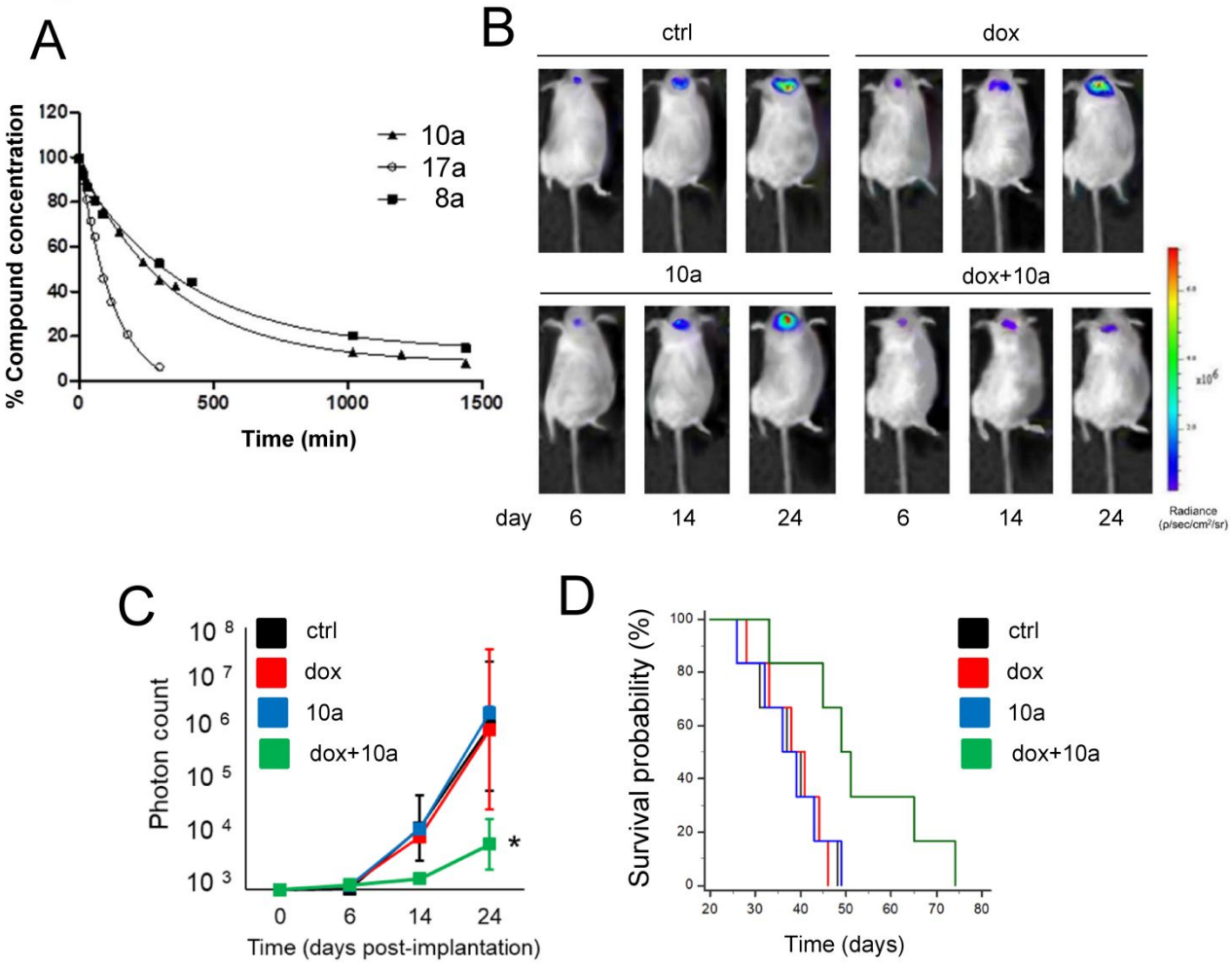

Biodistribution analysis indicated that – as expected – doxorubicin in plasma was progressively decreased, both in the absence or presence of **10a**, from 0.5 to 24 h. In mice treated with doxorubicin alone, the drug recovered in the brain was extremely low at each time point. Doxorubicin was mainly accumulated in liver, spleen and heart, followed by kidneys and lungs. Of note, in mice treated with doxorubicin and **10a** the decrease in plasma doxorubicin was faster and the drug became progressively detectable in brain extracts: the process was evident after 0.5 h, increased at 3 h and reached a steady-state at 6 h. By contrast, compound **10a** did not significantly changed the accumulation of doxorubicin within liver, spleen, heart, kidneys and lungs (**Figure 8**).

Figure 8

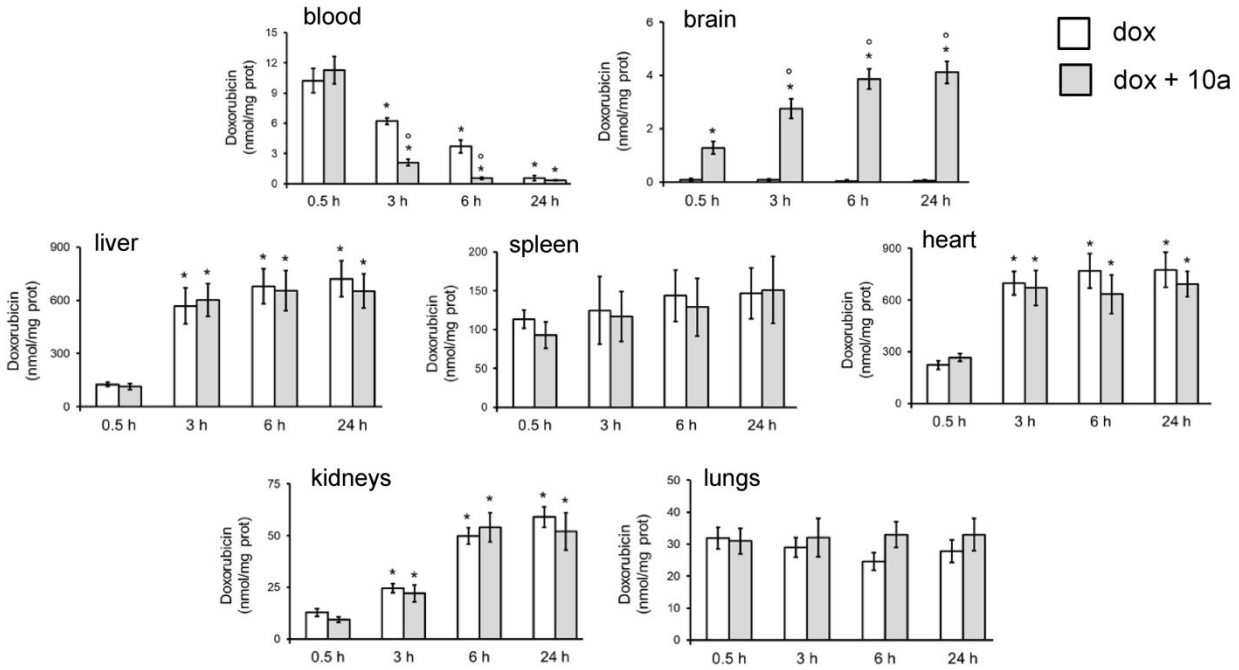

Since the biodistribution analysis highlighted a progressive accumulation of doxorubicin within brain parenchyma in animals treated with compound **10a** within the first 24 h, we analyzed the neuropathological impact of such accumulation. To this aim, a cohort of mice without GB – i.e. with an intact BBB – was treated with saline solution, doxorubicin, **10a** alone or in combination. Animals were sacrificed at one early time point (i.e. 24 h after treatments) and at one late time point (i.e. 7 days after treatments). While **10a** was detectable in the serum of animals 24 h after the administration, it was dramatically decreased after 7 days (**Figure 9A**). As expected, no doxorubicin was detectable within brain parenchyma in mice treated with the anthracycline only, likely because the drug does not cross BBB. Of note, in the group receiving doxorubicin + **10a**, doxorubicin was detectable in the brain parenchyma 24 h after the administration as indicated by the fluorescence microscopy analysis of the brain sections. The fluorescence disappeared in animals sacrificed 7 days after the treatments (**Figure 9B**). We next evaluated whether the amount of doxorubicin accumulated within the brain could induce any signs of toxicity. The cyto-architecture of cerebral cortex did not differ between each grop of treatments, both after 24 h and 7 days (**Figure 9C**), excluding structural damages.

Moreover, the amount of cleaved caspase 3 in the sections of animals treated doxorubicin + **10a** after 24 h and 7 days (i.e. the groups where we expected the maximal toxicity) was comparable to the amount detected in animals treated with saline solution (**Figure 9D**), excluding that the combination treatment induced neuronal apoptosis.

Figure 9

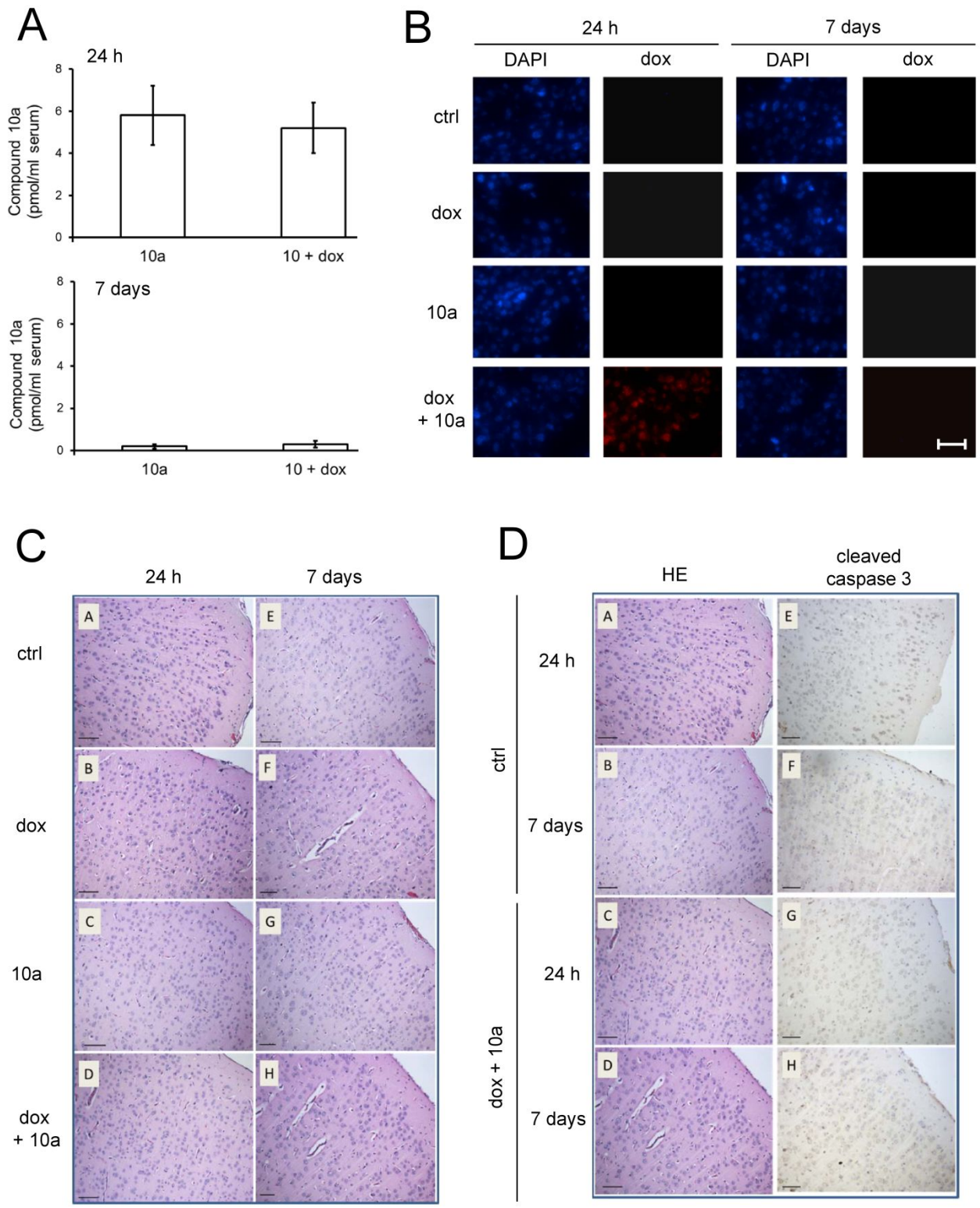

The absence of neuronal toxicity was paralleled by the absence of systemic toxicity. Indeed, in the blood of mice treated once/week for 3 weeks, the administration of compound **10a**, alone or combined with doxorubicin, did not increase the amounts of aspartate transaminase (AST), alanine transaminase

(ALT) and alkaline phosphatase (AP) – considered parameters of liver toxicity–, nor of creatinine – considered a parameter of kidney toxicity (**Table 1**). As expected, doxorubicin-treated mice had increased levels of creatine phosphokinase-MB (CPK-MB) and cardiac-troponin (c-TnT), two indexes of heart damage. **10a**, however, did not further increase these parameters, suggesting that it did not worsen the cardiac toxicity induced by doxorubicin (**Table 1**).

Table 1. Hematochemical parameters of the treated animals

Group	AST (U/L)	ALT (U/L)	AP (U/L)	creatinine (mg/L)	CPK-MB (ng/mL)	c-TnT (ng/mL)
ctrl	127 ± 56	38 ± 10	129 ± 39	0.041 ± 0.07	0.04 ± 0.01	0.010 ± 0.005
doxorubicin	157 ± 63	44 ± 12	129 ± 44	0.042 ± 0.009	0. 10± 0.02 *	0.032 ± 0.007 *
compound **10a**	126 ± 47	47 ± 9	139 ± 33	0.039 ± 0.008	0.03 ± 0.02 °	0.012 ± 0.004
doxorubicin + compound **10a**	171 ± 53	48 ± 13	138 ± 45	0.044 ± 0.010	0.09 ± 0.02 *	0.028 ± 0.005 *

Hematochemical parameters measured on animals treated as reported in Figure 7, on blood collected after euthanasia (day 25). AST: aspartate transaminase; ALT: alanine transaminase; AP: alkaline phosphatase; CPK-MB: creatine phosphokinase-MB; c-TnT: cacrdiac-troponin. Vs ctrl group: * $p < 0.005$.

Discussion

We propose three thiosemicarbazone compounds as effective inhibitors of Pgp acting at the same time in BBB and GB cells.

The compounds were selected from a larger library of collateral sensitivity inducers containing the 6,7-dimethoxytetrahydroisoquinoline basic moiety, responsible of Pgp modulation.[20] The thiosemicarbazones evaluated in the present study inhibited Pgp at nanomolar concentration and exerted cytotoxic activity at micromolar concentrations in cancer cell lines.[20] On the one hand this window made the compounds ineffective as potential antitumor agents or collateral sensitivity inducers. On the other hand, these features may grant a good therapeutic window. Most of Pgp

inhibitors successfully employed *in vitro* were ineffective in pre-clinical and clinical models for their undesired toxic effects at the concentrations used to achieve a detectable inhibition of Pgp.[31] According to our dose- and time-dependent cytotoxicity assays, the three compounds analyzed did not damage BBB cells nor reduced their viability when used at 10 nM for 3 h. This concentration and time were sufficient to inhibit Pgp, as demonstrated by the increased doxorubicin and rhodamine 123 uptake, and doxorubicin permeability across BBB monolayer. Although the increase in doxorubicin permeability was small, it was comparable to that produced by the last generation Pgp inhibitor Elacridar, suggesting that Pgp activity was abrogated in cells treated with thiosemicarbazone derivatives in these conditions. Moreover, at the same concentration, the compounds did not damage BBB integrity, as indicated by the lack of increase in dextran permeability and in TEER value, nor GB cells, as indicated by the lack of changes in extracellular LDH and cell viability. These data indicated that the ability to inhibit Pgp was coupled with the lack of toxicity on BBB and GB cells. Chemical or physical tight junctions opening [32,33], convection-enhanced delivery [34], craniotomy-based delivery and nanocarrier-based drug delivery [35], have been used to imporve drug delivery into CNS parenchyma, showing variable efficacy. Our approach differs from the current ones for at least two reasons.

First, thiosemicarbazones increased the permeability of Pgp substrates in a selective way. Indeed, the permeability of substrates of BCRP, another gatekeeper of BBB [36], the tight junctions competence and the TEER values were not changed. Such selectivity may limit eventual side-effects due to the broad alterations of BBB functions produced by other strategies. Moreover, the selective inhibition on Pgp was achieved at nanomolar concentration, in line with the most potent Pgp-inhibitors and Pgp-tracers used *in vivo*.[11,15]

Second, the increased uptake of doxorubicin in BBB and GB NS, when cultured alone, suggest that thiosemicarbazones may inhibit Pgp on both cell types. In GB/BBB co-culture setting, the increase in doxorubicin uptake was smaller in AC that had undetectable Pgp level than in NS, which had high

levels of Pgp. Of note, upon treatment with the compounds NS behaved like AC. If the effect of the compounds was limited to the inhibition of Pgp in BBB cells, we should expect that the increase in doxorubicin delivery remained higher in AC compared to NS co-cultured with BBB cells. We might hypothesize that the increase in doxorubicin accumulation and toxicity observed in BBB-GB co-cultures were not the simple consequence of an increased drug delivery across BBB, but it may be due to the simultaneous inhibition of Pgp on endothelial and tumor cells. This hypothesis was supported by the observation that all thiosemicarbazone derivatives were uptaken within BBB cells and crossed the BBB monolayer, although at a variable extent. Since the presence of BBB cells reduced the delivery of the compounds between the upper and lower chamber of Transwell devices to 40-60% of the amount present at t_0 in the upper chamber, we may hypothesize that part of the compounds is metabolized within BBB cells and/or retained within intracellular compartments, such as endosomes that slow the apical-basolateral transport of thiosemicarbazone derivatives. The amount of the compounds delivered across BBB was however sufficient to increase doxorubicin delivery and cytotoxicity against GB.

Since GB SC are rich of Pgp [6,37], which recognizes a large spectrum of chemotherapeutic drugs [9], the SC component is the hardest to be eradicated and is commonly responsible for tumor relapse or dissemination. The double inhibition of Pgp on BBB cells and likely on GB SC exerted by thiosemicarbazone compounds may amplify the anti-tumor efficacy of Pgp substrates like doxorubicin.

We are aware that doxorubicin is not the first-line therapy in GB: despite promising results *in vitro* [38], the extremely low delivery across BBB limits the use of doxorubicin in patients. However, given the relative sensitivity to doxorubicin of differentiated GB cells [38], several strategies aimed at improving doxorubicin efficacy are under evaluation in pre-clinical models and in clinical trials.[39-41] Our work demonstrated that thiosemicarbazones can transform doxorubicin, that does not cross BBB, into a BBB-permeant drug and effective even against GB SC. We next exploited the plasma stability

of the compounds, in order to use them in a preclinical setting. Compound **10a** was chosen as a compound coupling the highest permeability across BBB *in vitro* with a good stability in serum. In accord with the cytotoxicity results obtained in co-culture models, doxorubicin alone – at a cumulative dose that was significantly cardiotoxic in mice [42] – did not reduce the growth of orthotopically implanted GB SC-derived tumors. By contrast, doxorubicin efficacy was fully rescued by the co-administration with compound **10a,** as demonstrated by the decreased tumor growth and the increased median and overall survival in animals treated with doxorubicin + **10a**. Of note, the overall survival of the same strain of mice, orthotopically bearing the same tumor and treated with the first-line drug temozolomide, was 62 days, [43] i.e. lower than the survival of mice treated with doxorubicin + **10a** (74 days). Although these results were obtained in one single patient-derived xenograft, it is remarkable that this primary GB has high expression of Pgp and resistance to temozolomide, and a genetic and phenotypic profile indicative of high aggressiveness. [43] Our data suggest that doxorubicin + **10a** may be used as an alternative option to temozolomide in GB refractory to the first-line treatment. By screening more GB xenopatients, with different features in terms of chemoresistance and aggressiveness, we will likely obtain more specific indications on the genotypic/phenotypic profiles of GB that may have the greatest benefit from the combination of doxorubicin + thiosemicarbazone derivatives in terms of survival.

The biodistribution of doxorubicin was not significantly changed by **10a** in the typical sites of accumulation of the drug (liver, spleen and heart). However, the faster decrease of doxorubicin concentration from blood and the increase of doxorubicin within brain parenchyma – observed in mice treated with doxorubicin and **10a** – support the hypothesis that **10a** favored the transport of doxorubicin from bloodstream into brain parenchyma, by inhibiting Pgp present in BBB cells and reducing the brain-to-blood efflux of doxorubicin. The peculiar effect of **10a** can be explained by its tropism for BBB cells, as demonstrated by its ability of being accumulated within BBB cells and crossing BBB monolayer.

In accord with the half-life measured *ex vivo*, **10a** was detectable in the serum of animals within the first 24 h after the administration, but it was nearly undetectable after 7 days, i.e. immediately before the subsequent administration in our treatment protocol. We hypothesize that within 7 days **10a** was fully metabolized and/or excreted. An in depth characterization of the pharmacokinetic profile of **10a** is currently ongoing.

During the first 24 h, however, animals treated with **10a** progressively accumulated doxorubicin within the brain parenchyma. Of note, these results were obtained in animals without tumors, suggesting that **10a** was able to increase the delivery of doxorubicin across a physiologically intact BBB. If this effect was positive in terms of increased anti-tumor activity towards the GB cells present in the BAT area, it may produce undesired neurological toxicity. Our histopathological analysis, however, excluded that the doxorubicin accumulated altered the normal cyto-architecture of brain parenchyma or induced neuronal apoptosis. We hypothesize that – after the initial accumulation within the brain consequent to the increased delivery across BBB –doxorubicin was removed by cerebrospinal fluid, as suggested by the undetectable levels of the drug after 7 days from the administration. Thanks to this equilibrium of delivery and efflux, we hypothesized that doxorubicin concentration within the brain was kept under the neurotoxic threshold. The absence of neurological toxicity, coupled with the absence of systemic toxicity, according to the hematochemical parameters analyzed, suggest that **10a** has a safe pharmacological profile. In particular, the therapeutic benefit was not paralleled by any increase in doxorubicin cardiotoxicity, suggesting that the combination of doxorubicin plus the thiosemicarbazone was effective and well-tolerated.

These results may set the bases for the pre-clinical application of thiosemicarbazones, associated with doxorubicin and/or first-line and second-line chemotherapeutic drugs such as temozolomide, topoisomerase I and II inhibitors. These drugs are all substrate of Pgp [5,9] and have therefore limited efficacy against GB SC.[17]

Besides recognizing many chemotherapeutic drugs, Pgp limits the delivery to CNS of several analgesic, anti-inflammatory, antiviral and antiepileptic drugs.[9] In a broader perspective, our thiosemicarbazone compounds may be potentially used in the treatment of all those CNS diseases where Pgp represents an obstacle, including tumors, epilepsy and neurodegenerative diseases.

Conflict of interests disclosure

The authors declare no competing financial interest.

Acknowledgments

This work was supported by the Italian Association on Cancer Research (IG21408 to CR), Fondazione Italiana per la Ricerca sul Cancro (FIRC Fellowship to ICS), Italian Ministry of University and Research (FARB 2017 to CR).

References

1. Bai, R.Y.; Staedke, V.; Riggins, G.J. Molecular targeting of GB: Drug discovery and therapies. *Trends Mol. Med.* **2011**, *17*, 301–312.

2. Corso, C.D.; Bindra, R.S. Success and Failures of Combined Modalities in Glioblastoma Multiforme: Old Problems and New Directions. *Semin. Radiat. Oncol*. **2016**, *26*, 281–298.

3. Beier, D.; Schulz, J.B.; Beier C.P. Chemoresistance of glioblastoma cancer stem cells--much more complex than expected. *Mol. Cancer* **2011**, *10*, 128

4. Auffinger, B.; Spencer, D.; Pytel, P.; Ahmed, A.U.; Lesniak, M.S. The role of glioma stem cells in chemotherapy resistance and glioblastoma multiforme recurrence. *Expert. Rev. Neurother*. **2015**, *15*, 741–752.

5. Munoz, J.L.; Walker, N.D.; Scotto, K.W.; Rameshwar, P. Temozolomide competes for P-glycoprotein and contributes to chemoresistance in glioblastoma cells. *Cancer Lett*. **2015**, *367*, 69–75.

6. Nakai, E.; Park, K.; Yawata, T.; Chihara, T.; Kumazawa, A.; Nakabayashi, H.; Shimizu, K. Enhanced MDR1 Expression and Chemoresistance of Cancer Stem Cells Derived from GB. *Cancer Invest.* **2009**, *27*, 901–908.

7. Balik, V.; Mirossay, P.; Bohus, P.; Sulla, I.; Mirossay, L.; Sarissky, M. Flow Cytometry Analysis of Neural Differentiation Markers Expression in Human GBs May Predict Their Response to Chemotherapy. *Cell Mol. Neurobiol.* **2009**, *29*, 845–858.

8. Agarwal, S.; Sane, R.; Oberoi, R.; Ohlfest, J.R.; Elmquist, W.F. Delivery of molecularly targeted therapy to malignant glioma, a disease of the whole brain. *Expert Rev. Mol. Med.* **2011**, *13*, 17.

9. Pinzón-Daza, M.L.; Campia, .; Kopecka, J.; Garzón, R.; Ghigo, D.; Riganti, C. Nanoparticle- and liposome-carried drugs: new strategies for active targeting and drug delivery across blood-brain barrier. *Curr. Drug Metab*. **2013**, *14,* 625–640.

10. Zhou, Y.G.; Li, K.Y.; Li, H.D. Effect of the novel antipsychotic drug perospirone on P-glycoprotein function and expression in Caco-2 cells. *Eur. J. Clin. Pharmacol*. **2008**, *64*, 697–703.

11. Bauer, F.; Wanek, T.; Mairinger, S.; Stanek, J.; Sauberer, M.; Kuntner, C.; Parveen, Z.; Chiba, P.; Müller, M.; Langer, O.; Erker, T. Interaction of HM30181 with P-glycoprotein at the murine blood-brain barrier assessed with positron emission tomography. *Eur. J. Pharmacol*. **2012**, *696*, 18–27.

12. Pinzón-Daza, M.; Garzón, R.; Couraud, P.; Romero, I.; Weksler, B.; Ghigo, D.; Bosia, A.; Riganti, C. The association of statins plus LDL receptor-targeted liposome-encapsulated doxorubicin increases in vitro drug delivery across blood-brain barrier cells. *Br. J. Pharmacol*. **2012**, *167*, 1431–1447.

13. Riganti, C.; Salaroglio, I.C.; Pinzòn-Daza, M.L.; Caldera, V.; Campia, I.; Kopecka, J.; Mellai, M.; Annovazzi, L.; Couraud, P.O.; Bosia, A.; Ghigo, D.; Schiffer, D. Temozolomide down-regulates

P-glycoprotein in human blood-brain barrier cells by disrupting Wnt3 signaling. *Cell Mol. Life Sci*. **2014**, *71*, 499–516.

14. Pinzón-Daza, M.L.; Salaroglio, I.C.; Kopecka, J; Garzòn, R.; Couraud, P.O.; Ghigo, D.; Riganti, C. The cross-talk between canonical and non-canonical Wnt-dependent pathways regulates P-glycoprotein expression in human blood-brain barrier cells. *J. Cereb. Blood. Flow Metab*. **2014**, *34*, 1258–1269.

15. Bauer, M.; Karch, R.; Zeitlinger, M.; Philippe, C.; Römermann, K.; Stanek, J.; Maier-Salamon, A: Wadsak, W.; Jäger, W.; Hacker, M.; Müller, M.; Langer, O. Approaching complete inhibition of P-glycoprotein at the human blood-brain barrier: an (R)-[^{11}C]verapamil PET study. *J. Cereb. Blood Flow Metab.* 2015, 35, 743–746.

16. Agarwal, S.; Mittapalli, R.K.; Zellmer, D.M.; Gallardo, J.L.; Donelson, R.; Seiler, C.; Decker, S.A.;, SantaCruz, K.S.; Pokorny, J.L.; Sarkaria, J.N.; Elmquist, W.F.; Ohlfest, J.R. Active efflux of dasatinib from the brain limits efficacy against murine glioblastoma: broad implications for the clinical use of molecularly-targeted agents. *Mol. Cancer Ther.* **2012**, *11*, 2183–2192.

17. Riganti, C.; Salaroglio, I.C.; Caldera, V.; Campia, I.; Kopecka, J.; Mellai, M.; Annovazzi, L.; Bosia, A.; Ghigo, D.; Schiffer, D. Temozolomide downregulates P-glycoprotein expression in glioblastoma stem cells by interfering with the Wnt3a/glycogen synthase-3 kinase/β-catenin pathway. *Neuro Oncol*. **2013**, *15*, 1502–1517.

18. Sheehy, R.M.; Kuder, C.H.; Bachman, Z.; Hohl, R.J. Calcium and P-glycoprotein independent synergism between schweinfurthins and verapamil. *Cancer Biol. Ther*. **2015**, *8*, 1259–1268.

19. Szakács, G.; Hall, M.D.; Gottesman, M.M.; Boumendiel, A.; Kachadourian, R.; Day, B.J.; Baubichon-Cortay, H.; Di Pietro, A. Targeting the Achilles Heel of Multidrug-Resistant Cancer by Exploiting the Fitness Cost of Resistance. *Chem. Rev*. **2014**, *114*, 5753–5774-

20. Pati, M.L.; Niso, M.; Ferorelli, S.; Abate, C.; Berardi, F. Novel metal chelators thiosemicarbazones with activity at the σ_2 receptors and P-glycoprotein: an innovative strategy for resistant tumor treatment. *RSC Advances* **2015**, *5*, 103131–103146.

21. Richardson, D.R.; Sharpe, P.C.; Lovejoy, D.B.; Senaratne, D.; Kalinowski, D.S.; Islam, M.; Bernhardt, P.V. Dipyridyl thiosemicarbazone chelators with potent and selective antitumor activity form iron complexes with redox activity. *J. Med. Chem.* **2006**, *49*, 6510–6521.

22. Pluchino, K.M.; Hall, M.D.; Goldsborough, A.S.; Callaghan, R.; Gottesman, M.M. Collateral sensitivity as a strategy against cancer multidrug resistance. *Drug Resist. Updat*. **2012**, *15*, 98–105.

23. Weksler, B.B.; Subileau, E.A.; Perrière, N.; Charneau, P.; Holloway, K.; Leveque, M.; Tricoire-Leignel, H.; Nicotra, A.; Bourdoulous, S.; Turowski, P.; Male, D.K.; Roux, F.; Greenwood, J.; Romero, I.A.; Couraud, P.O. Blood-brain barrier-specific properties of a human adult brain endothelial cell line. *FASEB J.* **2005**, *19*, 1872–1894.

24. Abate, C.; Pati, M.L.; Contino, M.; Colabufo, N.A.; Perrone, R.; Niso, M.; Berardi, F. From mixed sigma-2 receptor/P-glycoprotein targeting agents to selective P-glycoprotein modulators: Small structural changes address the mechanism of interaction at the efflux pump. *Eur. J. Med. Chem.* **2015,** *89*, 606-615.

25. Reynolds, B.A.; Tetzlaff, W.; Weiss, S. A multipotent EGF-responsive striatal embryonic progenitor cell produces neurons and astrocytes. *J. Neurosci.* **1992**, *12,* 4565–4574.

26. Salaroglio, I.C.; Gazzano, E.; Kopecka, J.; Chegaev, K.; Costamagna, C.; Fruttero, R.; Guglielmo, S.; Riganti, C. New Tetrahydroisoquinoline Derivatives Overcome Pgp Activity in Brain-Blood Barrier and Glioblastoma Multiforme in Vitro. *Molecules* **2018**, *23*, 1401.

27. Riganti, C.; Miraglia, E.; Viarisio, D.; Costamagna, C.; Pescarmona, G.; Ghigo, D.; Bosia, A. Nitric oxide reverts the resistance to doxorubicin in human colon cancer cells by inhibiting the drug efflux. *Cancer Res*. **2005**, *65*, 516–525.

28. Monnaert, V.; Betbeder, D.; Fenart, L.; Bricout, H.; Lenfant, A.M.; Landry, C.; Cecchelli, R.; Monflier, E.; Tilloy. S. Effects of γ- and hydroxypropyl-γ-cyclodextrins on the transport of doxorubicin across an in vitro model of blood-brain barrier. *J. Pharmacol. Exp. Ther.* **2004**, *311*, 1115–1120.

29. Siflinger-Birnboim, A.; Del Vecchio, P.J.; Cooper, J.A.; Blumenstock, F.A.; Shepard, J.M.; Malik, A.B. Molecular sieving characteristics of the cultured endothelial monolayer. *J. Cell. Physiol.* **1987**, *132*, 111–117.

30. Colabufo, N.A.; Berardi, F.; Cantore, M.; Perrone, M.G.; Contino, M.; Inglese, C.; Niso, M.; Perrone, R.; Azzariti, A.; Simone, G.M.; Porcelli, L.; Paradiso, A. Small P-gp modulating molecules: SAR studies on tetrahydroisoquinoline derivatives. *Bioorg. Med. Chem*. **2008**, *16*, 362–373.

31. Callaghan, R.; Luk, F.; Bebawy, M. Inhibition of the multidrug resistance P-glycoprotein: time for a change of strategy? *Drug Metab. Dispos*. **2014**, *42*, 623–631.

32. Guillaume, D.J.; Doolittle, N.D.; Gahramanov, S.; Hedrick, N.A.; Delashaw, J.B.; Neuwelt, E.A. Intra-arterial chemotherapy with osmotic blood-brain barrier disruption for aggressive oligodendroglial tumors: results of a phase I study. *Neurosurgery* **2010**, *66*,48–58.

33. Liu, H-L.; Hua, M-Y.; Chen, P-Y.; Chu, P-C.; Pan, C-H.; Yang, H-W.; Wuang, C-Y.; Wang, J-J.; Yen, T-C.; Wei, K-C. Blood-brain barrier disruption with focused ultrasound enhanced delivery of chemotherapeutic drugs for glioblastoma treatment. *Radiology* **2010**, *255*, 415–425.

34. Jahangiri, A.; Chin, A.T.; Flanigan, P.M.; Chen, R.; Bankiewicz, K.; Aghi, M.K. Convection-enhanced delivery in glioblastoma: a review of preclinical and clinical studies. *J. Neurosurg*. **2016,** *1*, 1–10.

35. Karim, R.; Palazzo, C.; Evrard, B.; Piel, G. Nanocarriers for the treatment of glioblastoma multiforme: Current state-of-the-art. *J. Control. Release* **2016**, *227*, 23–37.

36. Agarwal, S.; Hartz, A.M.; Elmquist, W.F.; Bauer, B. Breast cancer resistance proteinand P-glycoprotein in brain cancer: two gatekeepers team up. *Curr. Pharm. Des*. **2011**, *17*, 2793–2802.

37. Salmaggi, A.; Boiardi, A.; Gelati, M.; Russo, A.; Calatozzolo, C.; Ciusani, E.; Sciacca, F.L.; Ottolina, A.; Parati, E.A.; La Porta, C.; Alessandri, G.; Marras, C.; Croci, D.; De Rossi, M. GB-Derived Tumorospheres Identify a Population of Tumor Stem-Like Cells with Angiogenic Potential and Enhanced Multidrug Resistance Phenotype. *Glia* **2006**, *54*, 850–860.

38. Hau, P.; Fabel, K.; Baumgart, U.; Rümmele, P.; Grauer, O.; Bock, A.; Dietmaier, C.; Dietmaier, W.; Dietrich, J.; Dudel, C.; Hübner, F.; Jauch, T.; Drechsel, E.; Kleiter, I.; Wismeth, C.; Zellner, A.; Brawanski, A.; Steinbrecher, A.; Marienhagen, J.; Bogdahn, U. Pegylated liposomal doxorubicin-efficacy in patients with recurrent high-grade glioma. *Cancer* **2004,** *100,* 1199–1207.

39. Kovacs, Z.; Werner, B.; Rassi, A.; Sass, J.O.; Martin-Fiori, E.; Bernasconi, M. Prolonged survival upon ultrasound-enhanced doxorubicin delivery in two syngenic glioblastoma mouse models. *J. Control. Release* **2014**, *187*, 74–82.

40. Mita, M.M.; Natale, R.B.; Wolin, E.M.; Laabs, B.; Dinh, H.; Wieland, S.; Levitt, D.J.; Mita, A-C. Pharmacokinetic study of aldoxorubicin in patients with solid tumors. *Invest. New Drugs*. **2015**, *33*, 341–348.

41. Whittle, J.R.; Lickliter, J.D.; Gan, H.K.; Scott, A.M.; Simes, .; Solomon, B.J.; MacDiarmid, J.; Brahmbhatt, H.; Rosenthal, M.A. First in human nanotechnology doxorubicin delivery system to target epidermal growth factor receptors in recurrent glioblastoma. *J. Clin. Neurosci*. **2015**, *22*, 1889–1894.

42. Gazzano, E.; Rolando, B.; Chegaev, K.; Salaroglio, I.C.; Kopecka, J.; Pedrini, I.; Saponara, S.; Sorge, M.; Buondonno, I.; Stella, B.; Marengo, A.; Valoti, M.; Brancaccio, M.; Fruttero, R.; Gasco, A; Arpicco, S.; Riganti, C. Folate-targeted liposomal nitrooxy-doxorubicin: An effective tool against P-glycoprotein-positive and folate receptor-positive tumors. *J. Control. Release* **2018,** *270*, 37–52.

43. Salaroglio, I.C.; Mujumdar, P.; Annovazzi, L.; Kopecka, J.; Mellai, M.; Schiffer, D.; Poulsen, S.A.; Riganti, C. Carbonic Anhydrase XII Inhibitors Overcome P-Glycoprotein-Mediated Resistance to Temozolomide in Glioblastoma. *Mol. Cancer Ther.* **2018**, *17*, 2598–2609.

Figure legends

Figure 1. Chemical structure of thiosemicarbazone derivatives

Figure 2. Cytotoxicity of thiosemicarbazone compounds on BBB cells

A-C. hCMEC/D3 cells were grown in the absence or in the presence of compounds **8a** (panel **A**), **10a** (panel **B**) and **17a** (panel **C**) at the indicated times and concentrations. The release of LDH (*left panels*) in the extracellular medium was measured spectrophotometrically, the cell viability (*right panels*)was measured by a chemiluminescence-based assay. Data are presented as means ± SD (n = 4). Versus untreated cells: * $p < 0.02$.

Figure 3. Effects of thiosemicarbazone compounds on BBB permeability

A-B. hCMEC/D3 cells were grown for 7 days up to confluence in Transwell inserts, then incubated 3 h with 5 μM doxorubicin (dox; panel **A**) or 10 μg/ml rhodamine 123 (panel **B**), alone or in the presence of 10 nM compounds **8a**, **10a** and **17a**. The intracellular retention of doxorubicin or rhodamine 123 was measured spectrofluorimetrically. Data are presented as means ± SD (n = 5). Versus dox: * $p < 0.002$. **C.** Scheme of the experimental assays of permeability. hCMEC/D3 (BBB) cells were grown for 7 days up to confluence in Transwell inserts, then incubated with thiosemicarbazones (yellow circles) plus doxorubicin (red triangles) or mitoxantrone (blue rhombusrs) or dextran-FITC (green squares). All the drugs were added in the upper chamber of the Trasnwell devices. After 3 h, the medium from the lower chamber was collected and the amount of doxorubicin, mitoxantrone or dextran-FITC was measured. **D-F.** hCMEC/D3 cells, grown as reportd in **C**, were incubated for 3 h with 5 μM doxorubicin (dox; panel **D**), 10 μM mitoxantrone (mxr; panel **E**), 2 μM dextran-FITC (dex; panel **F**), alone or in the presence of 10 nM compounds **8a**, **10a** and **17a**. When indicated, 10 μM Elacridar (**E**), was co-incubated with doxorubicin, as positive control of Pgp inhibition. The drug recovered from the lower chamber was measured fluorimetrically. Data are presented as means ± SD (n = 3). Vs dox: * $p < 0.001$. **G.** TEER values measured in hCMEC/D3

cells, grown for 7 days up to confluence in Transwell inserts and treated for 3 h with 10 nM compounds **8a**, **10a** and **17a**. Data are presented as means ± SD (n = 4).

Figure 4. Effects of thiosemicarbazone compounds on doxorubicin delivery in glioblastoma cells co-cultured with BBB cells

hCMEC/D3 cells were grown for 7 days up to confluence in Transwell inserts; 01010627 or CV17 adherent cells (AC) or stem cells (SC) were seeded at day 4 in the lower chamber. After 3 days of co-culture, supernatant in the upper chamber was replaced with fresh medium (ctrl) or with medium containing 5 μM doxorubicin (dox), in the absence or presence of 10 nM compounds **8a**, **10a** and **17a**. **A-B**. Fluorimetric quantification of intracellular doxorubicin in GB cells after 3 h. Data are presented as means ± SD (n = 3). Vs AC dox: * $p < 0.02$; vs SC dox: ° $p < 0.001$. **C.** 01010627 cells were seeded on sterile glass coverslips, treated as reported above, then stained with DAPI and analyzed by fluorescence microscopy to detect the intracellular accumulation of doxorubicin. Magnification: 63 x objective (1.4 numerical aperture); 10 x ocular lens. Bar: 10 μm. The micrographs are representative of 3 experiments with similar results.

Figure 5. Effects of thiosemicarbazone compounds on doxorubicin cytotoxicity in glioblastoma cells co-cultured with BBB cells

hCMEC/D3 cells were grown for 7 days up to confluence in Transwell inserts; 01010627 or CV17 adherent cells (AC) or stem cells (SC) were seeded at day 4 in the lower chamber. After 3 days of co-culture, supernatant in the upper chamber was replaced with fresh medium (ctrl) or with medium containing 5 μM doxorubicin (dox), in the absence or presence of 10 nM compounds **8a**, **10a** and **17a**. After changing the medium in the upper chamber, to remove any trace of the compounds, GB cells were let to grown for additional 24 h: the extracellular activity of LDH was checked spectrophotometrically (panel **A**, **C**), the cell viability was measured by a chemiluminescence-based

assay (panel **B, D**). Data are presented as means ± SD (n= 3). Vs AC/SC ctrl: * $p < 0.001$; vs AC/SC dox: ° $p < 0.001$; SC dox vs AC dox: # $p < 0.02$.

Figure 6. Pemeability of thiosemicarbazone compounds across BBB monolayer

hCMEC/D3 cells were grown for 7 days up to confluence in Transwell inserts, then incubated 3 h with 10 nM compounds **8a**, **10a** and **17a**. The amount of compounds within BBB cells (**panel A**) and in the lower chamber (**panel B-C**) was measured by RP-HPLC. The percentage of concentration of each compound in the lower chamber/concentration of each compound in the insert at t_0 (panel **B**) and the permeability coefficient (panel **C**) were calculated. Data are presented as means ± SD (n = 3).

Figure 7. Thiosemicarbazone derivatives improve doxorubicin efficacy against orthotopically implanted glioblastoma neurosphere-derived tumors

A. Half-lives of compounds **8a**, **10a** and **17a** in human plasma. Each point was performed in triplicate. The half-lives ($t_{1/2}$) of the compounds was determined by fitting the data with one phase exponential decay equation. **B.** Representative *in vivo* bioluminescence imaging of orthotopically implanted 01010627 NS, in animals treated with vehicle (ctrl), compound **10a** and doxorubicin (dox), as reported in the Experimental Section. **C.** Quantification of tumor-derived bioluminescence, taken as index of tumor growth. Data are presented as means±SD (6 animals/group). At day 24: * $p<0.01$: dox + **10a** group vs. all the other groups of treatment. **D.** Overall survival probability was calculated using the Kaplan-Meier method. $p<0.04$: dox + **10a** group vs. all the other groups of treatment (log rank test; not reported in the figure).

Figure 8. Thiosemicarbazone derivatives improve the doxorubicin distribution to the brain without inducing neuropathological damaging

A. BALB/c *nu*/*nu* mice were treated with 200 µl saline solution i.v. (used a a blank to subtract autofluorescence; not shown in the Figure), 5 mg/kg doxorubicin (dox; dissolved in 100 µl aqueous

solution) i.v., 5 mg/kg doxorubicin + 10 nM compound **10a** (dox+**10a**; dissolved on 100 µl aqueous solution with 1% DMSO) i.v. Animals were euthanized 0.5, 3, 6 and 24 h after treatments. The amount of doxorubicin was measured fluorimetrically in blood, brain, liver, spleen, heart, kidneys and lungs. Data are presented as means±SD (6 animals/group). * $p<0.05$: 3/6/24 h vs. 0.5 h; ° $p<0.001$: dox + **10a** group vs. dox group.

Figure 9. Thiosemicarbazone derivatives increase doxorubicin delivery to the brain without inducing apoptosis

BALB/c *nu*/*nu* mice were treated with 200 µl saline solution i.v. (ctrl), 5 mg/kg doxorubicin (dox; dissolved in 100 µl aqueous solution) i.v., 5 mg/kg doxorubicin + 10 nM compound **10a** (dox+**10a**; dissolved on 100 µl aqueous solution with 1% DMSO) i.v. Animals (n=6/group) were euthanized 24 h or 7 days after treatments. **A.** The amount of compounds within serum was measured by RP-HPLC. **B.** Brain slides were analyzed by fluorescence microscopy to measure the amount of doxorubicin. Nuclei were counterstained with DAPI. Bar: 10 µm. The micrographs are representative of 3 animals/group. **C-D.** Brain slides were stained with hematoxylin and eosin (HE; panels **C-D**) or immuno-stained for cleaved caspase 3 (panel **D**). Bar: 100 µm. The micrographs are representative of 3 animals/group.

Supporting information

Supplementary Figure 1. Expression of ABC transporters and tight junctions-related proteins in BBB cells

Supplementary Figure 2. Cytotoxic effects of doxorubicin and thiosemicarbazones on BBB cells

Supplementary Figure 3. Expression of ABC transporters in glioblastoma cells

Supplementary Figure 4. Doxorubicin uptake in glioblastoma cells

Supplementary Table 1. Histological characterization of AC and SC glioblastoma cells

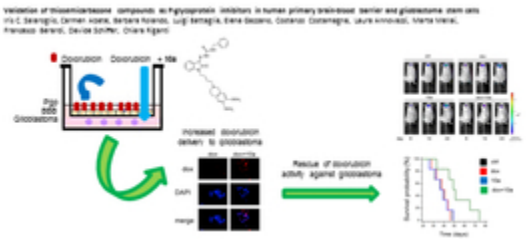

Graphical abstract

22x9mm (300 x 300 DPI)

Figure 1

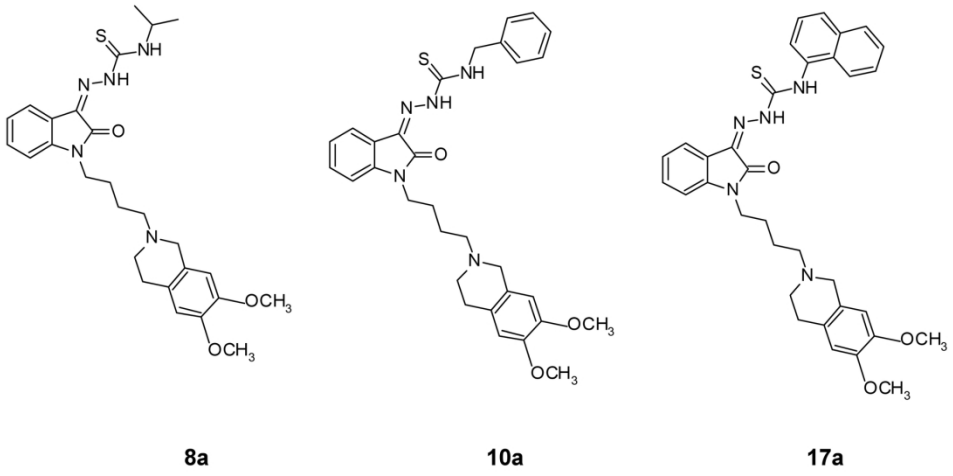

Figure 1

176x100mm (300 x 300 DPI)

Figure 2

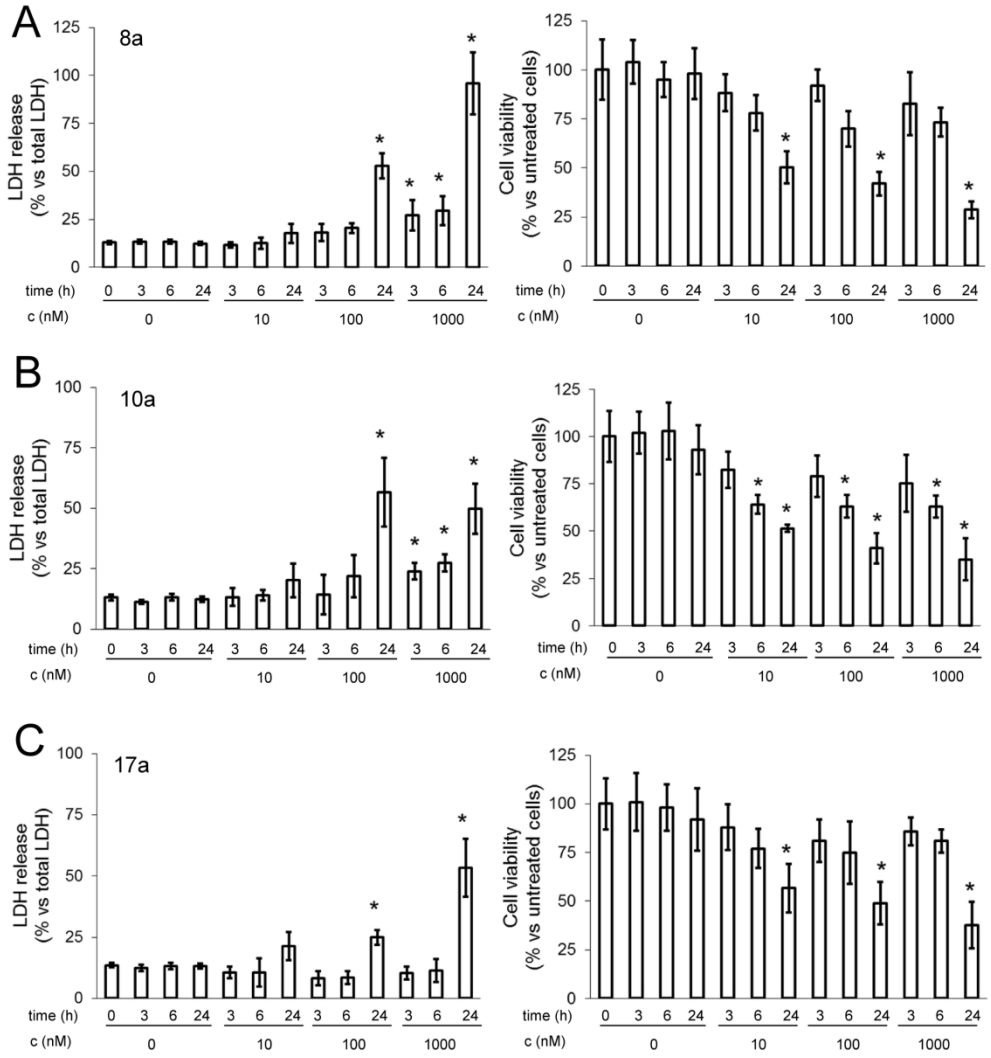

Figure 2

176x200mm (300 x 300 DPI)

Figure 3

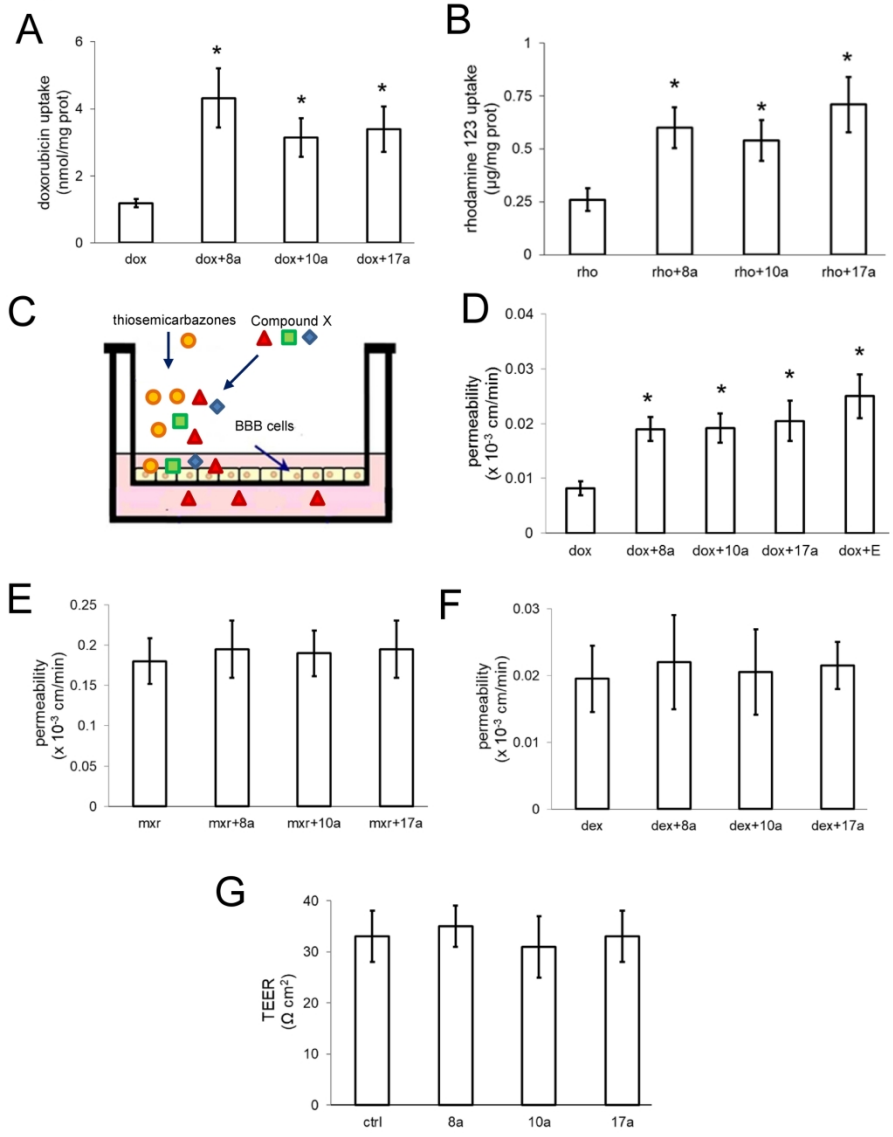

Figure 3

176x231mm (300 x 300 DPI)

Figure 4

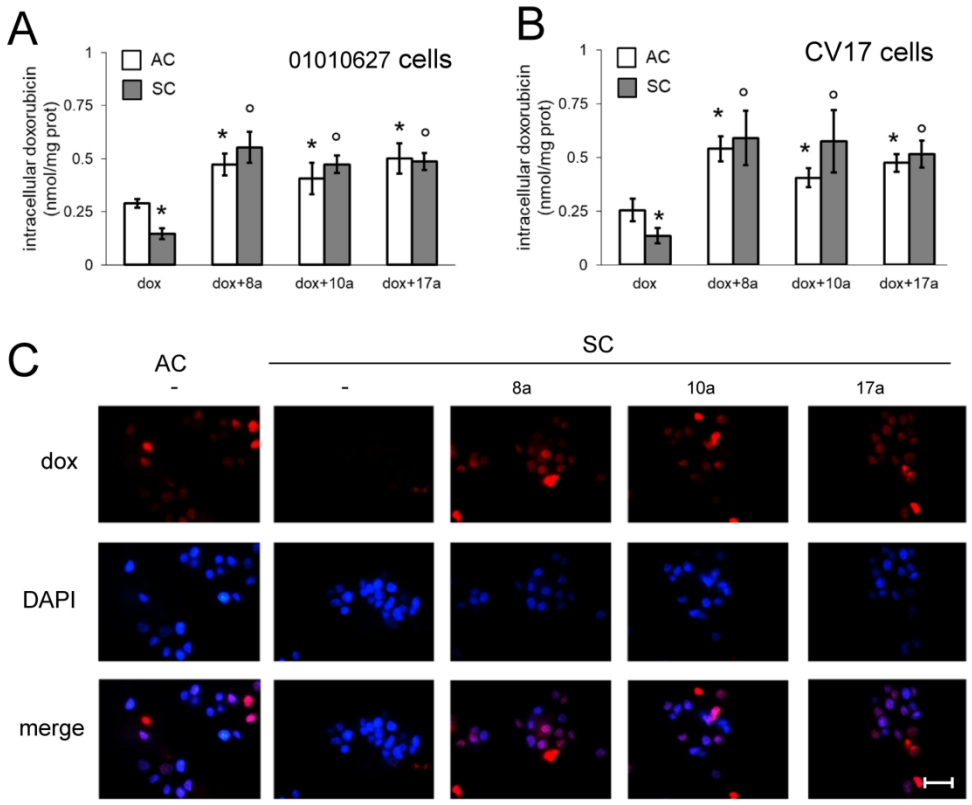

Figure 4

176x156mm (300 x 300 DPI)

Figure 5

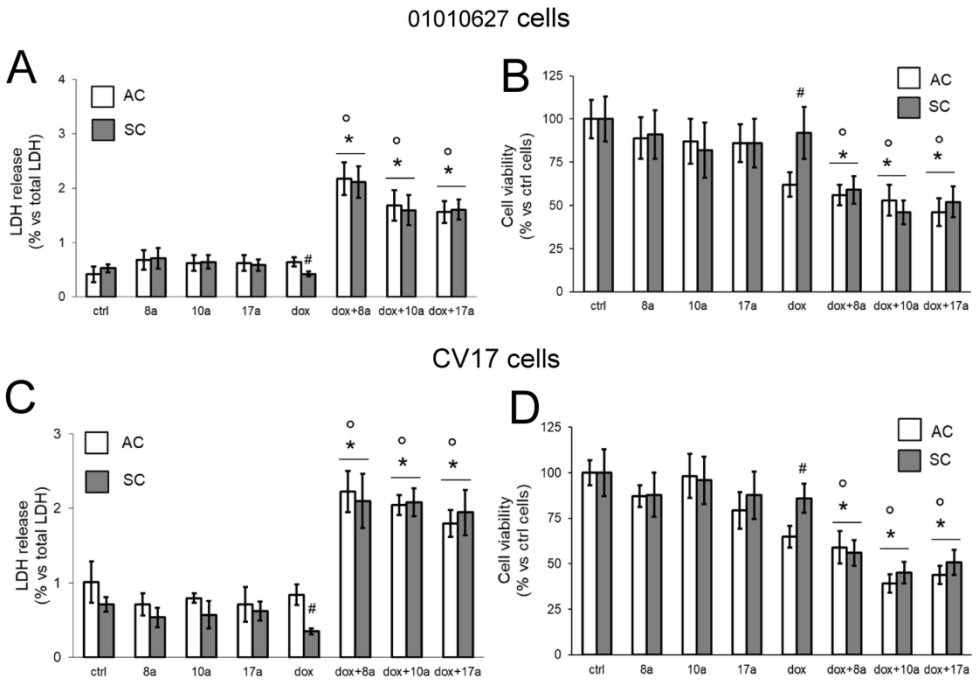

Figure 5

176x132mm (300 x 300 DPI)

Figure 6

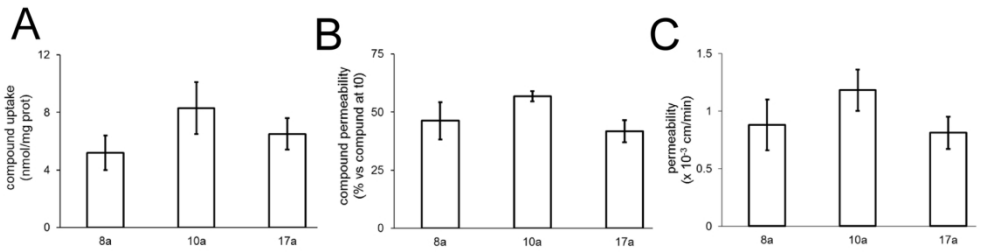

Figure 6

176x61mm (300 x 300 DPI)

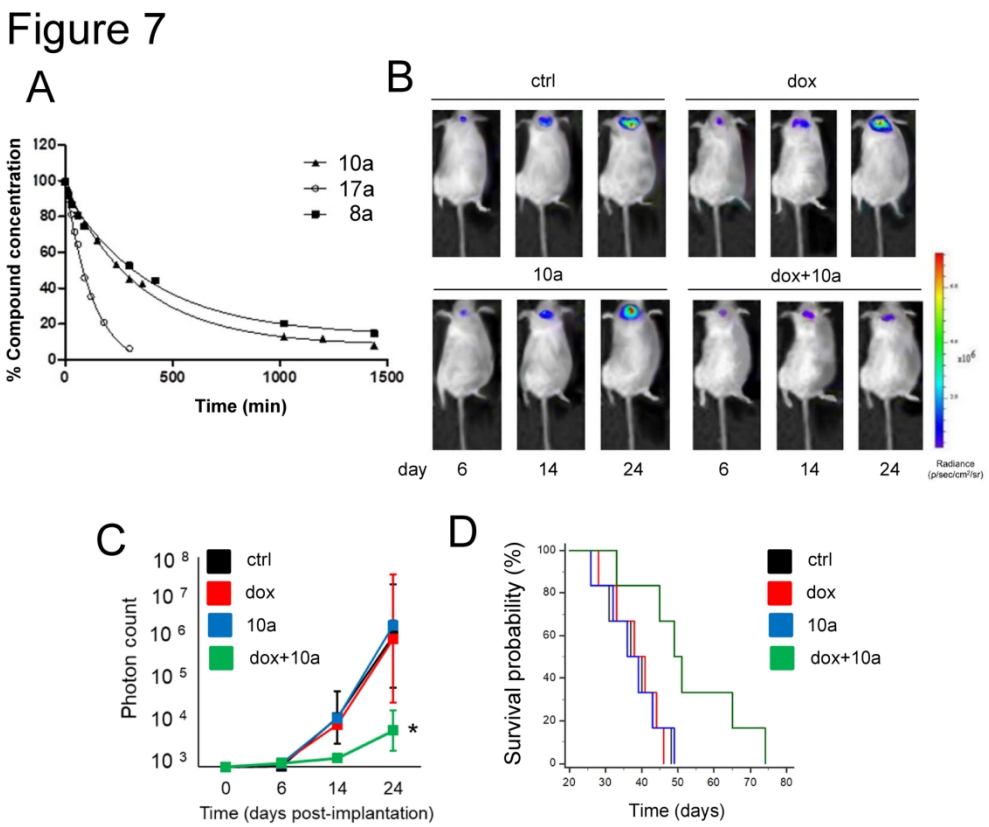

Figure 7

176x147mm (300 x 300 DPI)

Figure 8

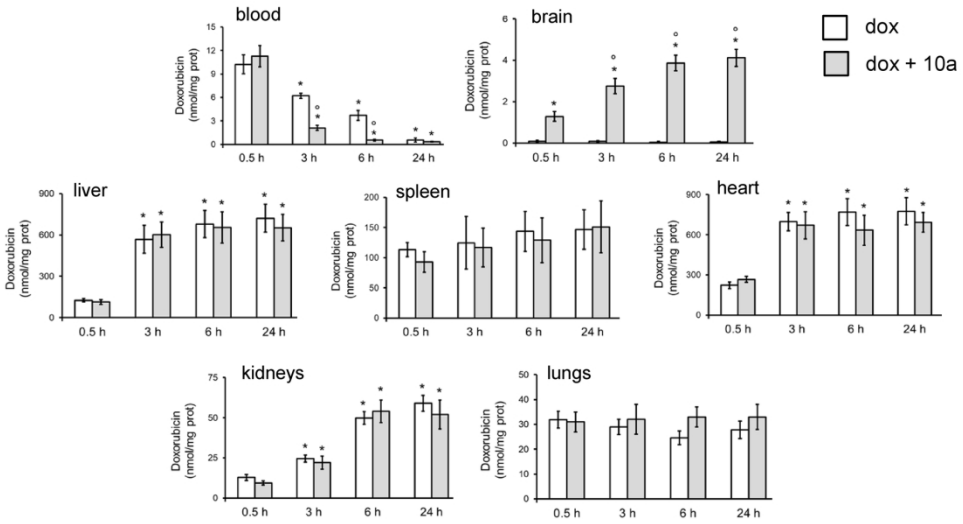

Figure 8

176x110mm (300 x 300 DPI)

Figure 9

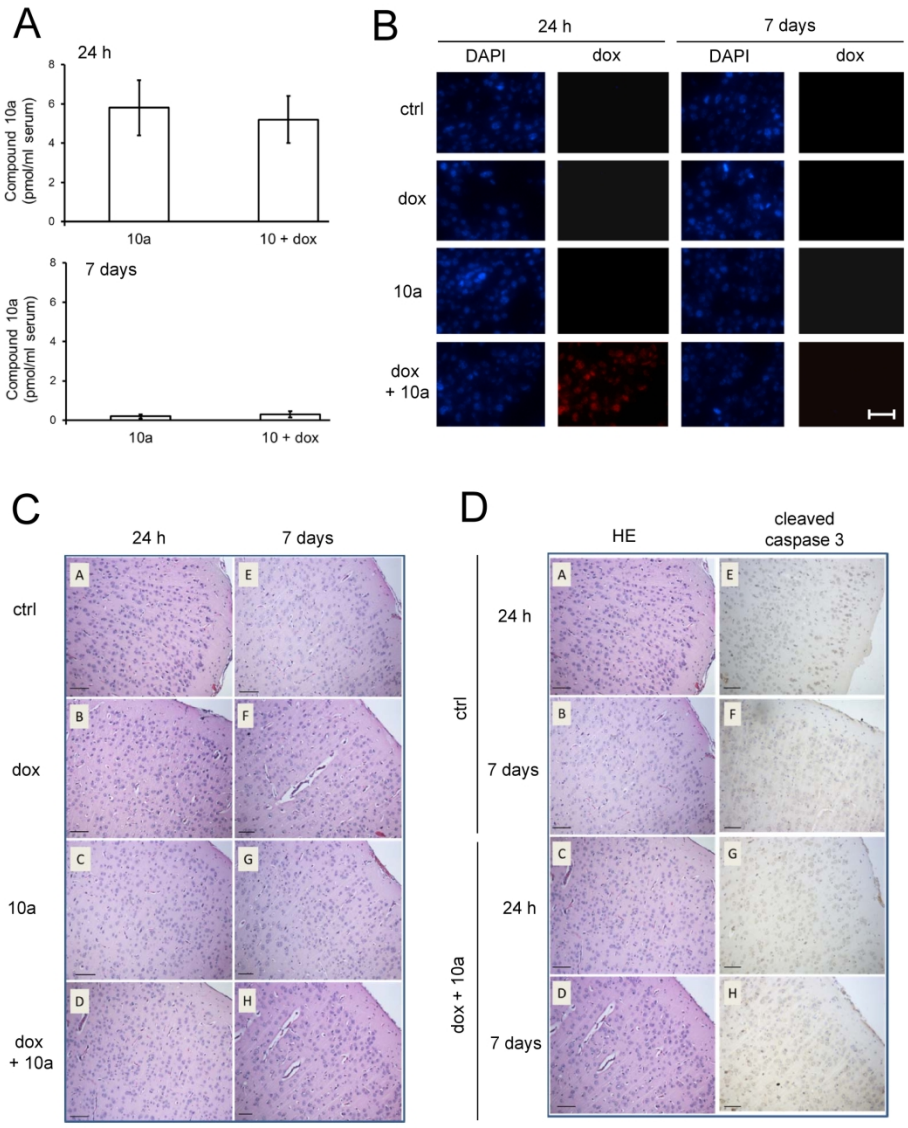

Figure 9

188x241mm (300 x 300 DPI)